Thesis for the Degree of Master of Science

Isolation of phytochemicals from red kohlrabi (*Brassica oleracea* var. *gongylodes*) tuber

by

Ritu Prajapati

Department of Food and Life Science

The Graduate School

Pukyong National University

August, 2020

Isolation of phytochemicals from red kohlrabi (*Brassica oleracea* var. *gongylodes*) tuber

적콜라비의 식물화학물질 분리

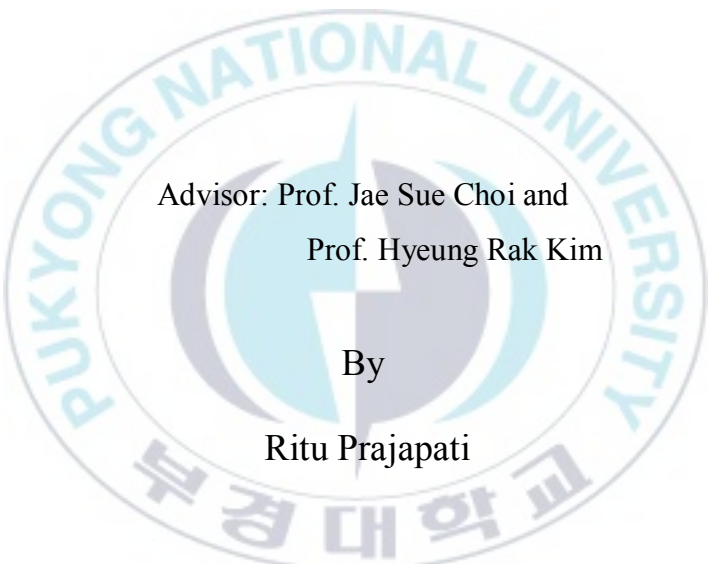

Advisor: Prof. Jae Sue Choi and
Prof. Hyeung Rak Kim

By

Ritu Prajapati

A thesis submitted in partial fulfillment of the requirements for the degree of

Master of Science

Department of Food and Life Science, The Graduate School

Pukyong National University

August 2020

Isolation of phytochemicals from red kohlrabi (*Brassica oleracea* var. *gongylodes*) tuber

A dissertation

by

Ritu Prajapati

Approved by:

(Chairman)

(Member)

(Member)

August, 2020

CONTENTS

Table

List of schemes

List of figures

Abbreviations

^{13}C NMR: Carbon 13 nuclear magnetic resonance

^{1}H NMR: Proton nuclear magnetic resonance

B. *oleracea*: *Brassica oleracea*

C/EBPα: CCAAT/ Enhancer-binding Protein α

Ca: Calcium

CC: Column chromatography

CH_2Cl_2: Dichloromethane

CH_3OH: Methanol

Cu: Copper

EIMS: Electron impact ionization mass spectrometry

ESIMS: Electrospray ionization mass spectrometry

EtOAc: Ethyl Acetate

Fe: Iron

HMBC: Heteronuclear multiple bond correlation

HMQC: Heteronuclear multiple quantum coherence

Hz: Hertz

J: Coupling constant

K: Potassium

MEK / ERK: Mitogen-activated protein kinase / Extracellular Signal-Regulated Kinase

MeOH: Methanol

Mg: Magnesium

Mn: Manganese

MTT: 3-(4, 5-dimethylthiazol-2-yl)-2, 5-diphenyl tetrazolium bromide

Na: Sodium

P: Phosphorus

PIP3-Akt-mTOR: Phosphatidylinositol (3, 4, 5)-trisphosphate-Protein kinase B- mammalian target of rapamycin

PPAR γ: peroxisome proliferator-activated receptor γ

RAE: Retinol activity equivalent

RP: Reverse phase

Se: Selenium

SiO2: Silica

SREBP-1: Sterol regulatory element-binding transcription factor 1

TLC: Thin layer chromatography

USDA: United States Department of Agriculture

UV: Ultraviolet

Zn: Zinc

적콜라비의 식물화학물질 분리

Ritu Prajapati

부경대학교 대학원 식품생명과학과

요 약

붉은 콜라비 (*Brassica oleracea* var. *gongylodes*)는 줄기와 뿌리가 식용 가능하며 전세계적으로 널리 소비되는 식물이다. 적콜라비의 양경 부분을 건조시킨 후 메탄올로 추출하였으며 농축한 추출물을 디클로로메탄 (CH_2Cl_2), 에틸아세테이트 (EtOAc), 그리고 물 (H_2O)의 순서로 분획하였다. 적콜라비의 에틸아세테이트 추출물로부터 11개의 화합물이 분리되었으며 그 중 화합물 1은 당화 인돌 알칼로이드 파생물질인 1-methoxyindole 3-carboxylic acid 6-*O*- β-D-glucopyranoside이며 이전에 보고된 바가 없다. 세파덱스 (sephadex) LH-2-과 RP-18을 이용한 EtOAc 분획물의 분리를 통해, 알려진 화합물인 β-Sitosterol glucoside (4), 5-hydroxymethyl-2-furaldehyde (5), methyl-1-thio-β-D-glucopyranosyl disulfide (6), 5-Hydroxy-2-pyridinemethanol (7), (3S, 4R)-2-Deoxyribolactone (8), *n*-Butyl-β-D-fructopyranoside (9), uridine (10) 그리고 세 개의 과당 파생 물질 tagatose (11), β-D-fructofuranose (12) 그리고 β-D-fructopyranose (13)를 수득하였다. CH_2Cl_2 분획물로부터는 두가지의 알려진 인돌 알칼로이드인 indole 3-acetonitrile (2) 그리고 N-methoxyindole 3-acetonitrile (3)를 분리하였다. 화학 구조는 ^{13}C 와 ^{1}H NMR, HMBC, HMQC, EIMS, HR-ESIMS, 선광도와 TLC의 비교, 그리고 문헌 참고를 통해 규명하였다. 화합물 2, 3, 4, 5, 6, 7, 8 그리고 9 는 콜라비로부터 처음으로 분리되었다.

1. Introduction

Increasing data on the health promoting properties of plants belonging to Brassicaceae has led to the upsurge in the consumption of these vegetables. *Brassica* vegetables constitute an essential part of human diet, and are rich sources of nutrients and health benefitting phytoconstituents such as vitamins, minerals, carbohydrates, amino acids, tocopherols, glucosinolates, carotenoids, and phenolic compounds (Park et al., 2013). Numerous studies have indicated the beneficial effects of *Brassica* vegetables associated with prevention of various diseases including diabetes, cancer and cardiovascular diseases (Ambrosone and Tang, 2009; Park et al., 2017). The cancer preventive roles of these vegetables are attributed to the presence of glucosinolates whose active metabolites such as isothiocyanates and indole derivatives modulate biotransformation enzyme system (Lampe and Peterson, 2002), while prevention of chronic diseases are offered through the reduction of oxidative stress by dietary antioxidants such as vitamin C, carotenoids, vitamin E and phenolic compounds (Podsędek, 2007).

Red kohlrabi (*Brassica oleracea* var. *gongylodes*), also known as German cabbage or cabbage turnip or turnip kale, is a minor crop that grows as an annual or a biennial crop with unbranched, shortened, swollen, sub-globose to globose, fleshy bulbotuber-like stem and highly branched root system. Though the cultivation of kohlrabi was reported to origin in north-western Europe, it is now produced in Europe, North America, Canada and several parts of Asia. Two types of kohlrabi cultivars are common, pale green and purple/red. The edible parts of the plant comprise of fleshy stem and leaves that are consumed either raw as salads or cooked as curry (Choi et al., 2010;

Lim, 2014). Unlike other Brassica vegetables, the stem of kohlrabi are generally eaten due to their sweetness, crispiness, and lower bitterness and pungency which enhance palatability of food (Choi et al., 2010).

Different studies have illustrated the nutritive and pharmacological benefits of kohlrabi, correlated with the primary and secondary metabolites of the plant (Lim, 2014; Park et al., 2012). According to USDA nutrition database (https://fdc.nal.usda.gov/fdc-app.html#/food-details/168424/nutrients), per 100 g of edible raw kohlrabi stem consists of approximately 91 g of water, 27 kcal energy, 1.7 g protein, 1.01 g total lipid, 1 g ash, 2.6 g total sugars, minerals like Ca (24 mg), Fe (0.04 mg), Mg (19 mg), P (46 mg), K (350 mg), Na (20 mg), Zn (0.03 mg), Cu (0.129 mg), Mn (0.139 mg) and Se (0.7 µg), vitamins such as Vitamin C (62 mg), thiamine (0.05 mg), riboflavin (0.02 mg), niacin (0.4 mg), pantothenic acid (0.165 mg), vitamin B6 (0.15 mg), total folate (16 µg), total choline (12.3 mg), vitamin A (2 µg RAE), vitamin E (0.48 mg), carotene (22 µg) and vitamin K (0.1 µg), along with other total saturated fatty acids (0.013 g), total mono- and poly-unsaturated fatty acid (0.055 mg), and amino acids such as tryptophan (0.010 g), threonine (0.049 g), isoleucine (0.078 g), leucine (0.067 g), lysine (0.056 g), methionine (0.013 g), cysteine (0.007 g), phenylalanine (0.039 g), valine (0.05 g), arginine (0.105 g), and histidine (0.019 g) (Agriculture, 2019; Lim, 2014). Park et al., 2017 identified a total of 45 compounds, comprising of primary metabolites such as amino acids, organic acids, carbohydrates, sugar alcohols and amine in pale green and purple kohlrabi by GC-MS approach. In addition, they found 11 anthocyanins, with cyanidin-3-(feruoyl)-diglucoside-5-glucoside being the dominant one (0.11 ± 0.00 mg/g DW), in purple cultivar. These coloring pigments were not detected in pale green cultivar. They found that purple kohlrabi had the greater amount of malate, fumarate, shikimate and tryptophan that serve as

precursors for many aromatic molecules like flavonoids, glucosinolates, phenolic acids and anthocyanins (Park et al., 2017).

Besides these, eight different glucosinolates were identified in green and purple kohlrabi cultivars, where glucoerucin was the major one in purple cultivars (2.06 μmol/g DW in skin and 8.08 μmol/g DW in flesh part of tuber) while glucotropeoline occurred in higher amount in green kohlrabi (0.94 μmol/g DW in skin and 4.27 μmol/g DW in flesh part of tuber). Carotenoids like β-carotene and lutein, and seven phenylpropanoids, namely, 4-hydroxycinnamic acid, caffeic acid, p-coumaric acid, benzoic acid, trans-cinnamic acid, quercetin and kaemferol, were also identified by GC-MS. Altogether, purple kohlrabi contained greater amount of these bioactive components than green kohlrabi, with total glucosinolates 18.98 μmol/g and 11.35 μmol/g, total anthocyanins 1.75 μmol/g and 0 μmol/g, total carotenoids 2.10 μg/g and 0.85 μg/g and total phenylpropanoids 47.75 mg/g and 49.07 mg/g, as measured for per gram of dry weight of the purple and the green kohlrabi's flesh respectively (Park et al., 2012). Since kohlrabi has its native odor and flavor, the volatile constituents in the stem were studied by Fischer in 1992. It was known that these volatiles consist of the sulfur and the nitrogen containing compounds, and in connection to the relative abundance and threshold concentration of volatiles, 3-methylthiopropyl, 4-methylthiobutyl and allyl isothiocynate were found to be the major constituents (Fischer, 1992). However, the appearance and proportions of different constituents in the plant varies depending on the agronomic conditions such as cultivars, fertilizers, plant organ, developmental stage, climatic condition, light and water regime (Björkman et al., 2011).

Previously, Jung et al. demonstrated anti-diabetic, anti-inflammatory and anti-oxidant effects of the methanolic extract of red and green kohlrabi

cultivars and on comparison, they found the red kohlrabi extract to have more significant effect (Jung et al., 2014). Likewise, kohlrabi was shown to be anti-adipogenic (Lee et al., 2014), anti-hyperglycemic (Sharma et al., 2015), anti-hyperlipidemic (Sharma et al., 2015), anti-oxidant (Kim et al., 2014; Sharma et al., 2015; Yang et al., 2015; Yi et al., 2017) and anti-proliferative (Yang et al., 2015). These pharmacological advantages of kohlrabi can be ascribed to its constitutive phytochemicals.

The metabolic profiling of the kohlrabi extract has assisted in understanding the general composition of kohlrabi cultivars, however, phytochemical studies of *B. oleracea* var. *gongylodes* involving the isolation of compounds are scarce. Though numerous studies are available on the compounds derived from vegetables of *Brassica* genus, the investigations on the phytoconstituents have yet to offer the identification of more compounds. UV-treatment as well as the supplementation of radioactive L- [β-^{14}C] tryptophan and L-[$^{14}CH_3$] methionine to UV-irradiated stem tuber of kohlrabi provided six distinguishable phytoalexins in the chloroform extract of treated tuber, namely, methoxybrassitin, methoxybrassinin, cyclobrassinin, cyclobrassinon, spirobrassinin and 1-methoxyspirobrassinin (Gross et al., 1994). Column chromatography (CC) of ethyl acetate faction of methanol extract resulted in the isolation of three sterols, β-sitosterol, brassicasterol and ketobrassicasterol (Lee, J.-W. et al., 2010). From butanol fraction of kohlrabi sprouts, Lee et al. (2014) isolated four phenylpropanoids, which are 3-(3, 4, 5-trimethoxyphenyl)-2*E*-propenoic acid methyl ester (**a**), (*E*)-sinapic acid methyl ester (**b**), (*E*)-sinapoyl glucoside (**c**) and lawsoniaside B (**d**). Of these, three compounds (**a**, **c** and **d**) exhibited significant inhibition on nitric oxide production in raw 264.7 macrophage cells, thus indicating the anti-inflammatory effect.

As different phytochemical researches have added chemical diversity in the existing pool of bioactive compounds, providing more molecules for pharmacological screening, natural products investigation in the edible flora draws considerable attention. This present study aimed to investigate the chemical constituents of red kohlrabi's stem tuber. Repeated column chromatography of the EtOAc fraction of methanolic extract of kohlrabi tuber led to the isolation of a new glycoside derivative of indole alkaloid, 1-methoxyindole 3-carboxylic acid 6-*O*- β-D-glucopyranoside (**1**), whose structure was determined using spectroscopic analyses. In addition, nine known compounds viz. indole 3-acetonitrile (**2**), N-methoxyindole 3-acetonitrile (**3**), β-sitosterol glucoside (**4**), 5-hydroxymethyl-2-furaldehyde (**5**), methyl-1-thio-β-D-glucopyranosyl disulfide (**6**), 5-hydroxy-2-pyridinemethanol (**7**), (3S, 4R)-2-deoxyribolactone (**8**), *n*-butyl-β-D-fructopyranoside (**9**), uridine (**10**) and three fructose derivatives, tagatose (**11**), β-D-fructofuranose (**12**) and β-D-fructopyranose (**13**) were isolated.

2. Materials and methods

2.1 Plant material

Red/ purple kohlrabi tubers *(B. oleracea* var. *gongylodes*) were bought from a local retailer and authenticated by Prof. Jae Sue Choi (Pukyong National University, Busan, South Korea). A voucher specimen 20131029 was deposited in the authorized laboratory (J.S. Choi).

2.2 General experimental procedures

^{1}H and ^{13}C NMR spectra were recorded using JEOL JNM ECP-600/400 spectrometer (Tokyo, Japan) at 600 MHz and 400 MHz using deuterated methanol (CD_3OD) and pyridine (C_5D_5N). HR-ESI-MS spectra was obtained from a JEOL JMS-700 spectrometer (Tokyo, Japan). EIMS was recorded using GCMS QP-2010 Ultra (Shimadzu, Japan). Optical rotation was determined using P-2000 polarimeter (JASCO, Japan). FTIR was measured with FT-4100 (JASCO, Japan). UV/Vis absorption was measured using Biochrom Libra S22 UV/Vis spectrophotometer. Column chromatography (CC) was conducted using silica (SiO_2) gel 60 (70-230 mesh, Merck, Darmstadt, Germany), sephadex LH-20 (20-100 µM, Sigma, St. Louis, MO, USA) and LiChroprep RP-18 (40-63 µM, Merck, Darmstadt, Germany). Thin layer chromatography (TLC) was performed with precoated Merck Kiesel gel 60 F_{254} plates and RP-18 F_{254S} plates, using 25% sulfuric acid as spray reagent for heating. TLC plates were visualized in UV chamber (UVItec, Cambridge CB4 1QB, UK) at 365 nm and 254 nm. All solvents used for CC were of reagent grade and purchased from commercial suppliers.

2.3 Experimental methods

2.3.1 Extraction and fractionation

Extract of red kohlrabi tuber (754.13 g) was obtained by refluxing 5.0 kg of sliced tuber in methanol (CH_3OH) for 3 hours (5L x 2 times) and drying using rotatory vacuum evaporator at 40 °C (Laborota 4000, Heidolph, Germany). The dried methanolic extract was suspended in distilled water (H_2O) and partitioned successively with dichloromethane (CH_2Cl_2), ethyl acetate (EtOAc) and *n*-butanol (*n*-BuOH) to yield CH_2Cl_2 (2.1 g), EtOAc (14.5 g) and *n*-BuOH (30.38 g) fractions.(Scheme 1)

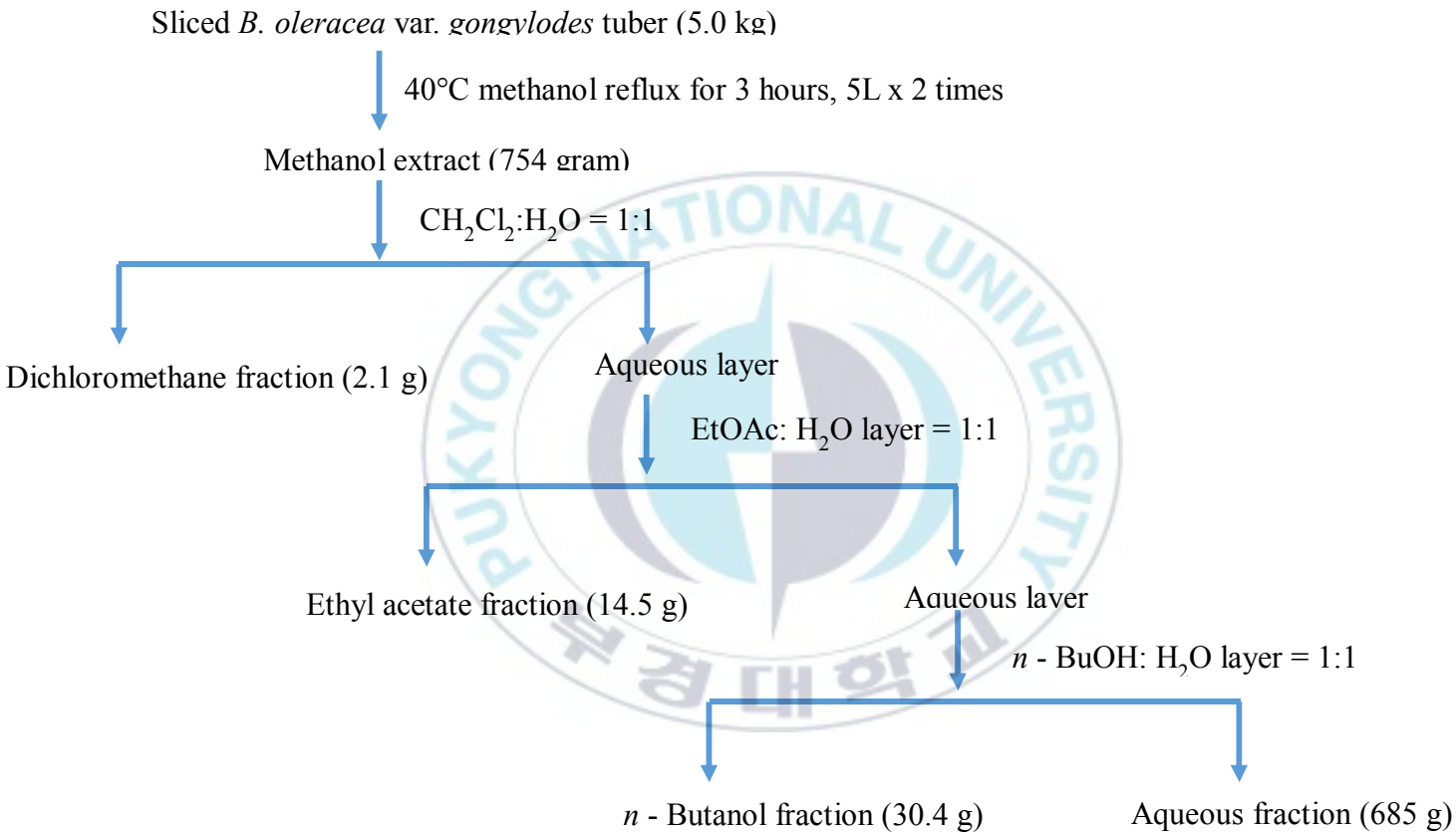

Scheme 1. Extraction and fractionation procedure of raw *B. oleracea* var. *gongylodes* tuber.

2.3.2 Isolation and identification

EtOAc fraction (14.5 g) was subjected for normal phase silica gel column chromatography (CC) using stepwise gradient elution of CH_2Cl_2: CH_3OH: H_2O from 10:1:0.1 to 2:1:0.1 to 0:1:0, v/v/v, to give eight sub-fractions (SF). (Scheme 2)

SF-2 (1.4 g) was chromatographed using SiO_2 gel with successive increase in polarity of hexane: ethyl acetate (H: E 7:1 →1:1) solvent system and purified using sephadex LH20 and RP-18 to obtain compounds **4** (36 mg) and **5** (120 mg). Repeated CC of SF-3 (1.15 g) through SiO_2, RP-18 and sephadex LH-20 gave **8** (120 mg). From SF-4 (1.20 g), compounds **6** (200 mg) and **7** (20 mg) were isolated by running through RP-18 gel using 50% - 0% CH_3OH and purified by using silica gel using CH_2Cl_2: CH_3OH: H_2O 10:1:0.1. SF-5 (3.13 g) was chromatographed through sephadex LH-20 using methanol and the resulting sub-fractions were run through SiO_2 gel using EtOAc: CH_3OH: H_2O 40:1→ 24:4:3 to separate compounds **1** (12 mg), **9** (32 mg) and **10** (10 mg), which were purified by eluting through RP-18 gel. Repeated CC using 50 % - 20% CH_3OH for RP gel and EtOAc: CH_3OH: H_2O 20:1 →21:5:3 of SF-6 (1.23 g) further yielded compounds **11**(85 mg) and **12** (36 mg). Likewise, SF-7 (2.61 g) when chromatographed through SiO_2 gel using EtOAc: CH_3OH: H_2O and purified by eluting through RP-18 and sephadex LH-20 with increasing concentration of methanol gave **13** (650 mg).

CH_2Cl_2 fraction when chromatographed using SiO_2 gel with gradient elution by H:E 50:1 gave eight sub-fractions. D-SF-8 and D-SF-3 by repeated column chromatography using SiO_2 gel and sephadex LH-20 resulted in the isolation **2** (8 mg) and **3** (6 mg) respectively (Scheme 3).

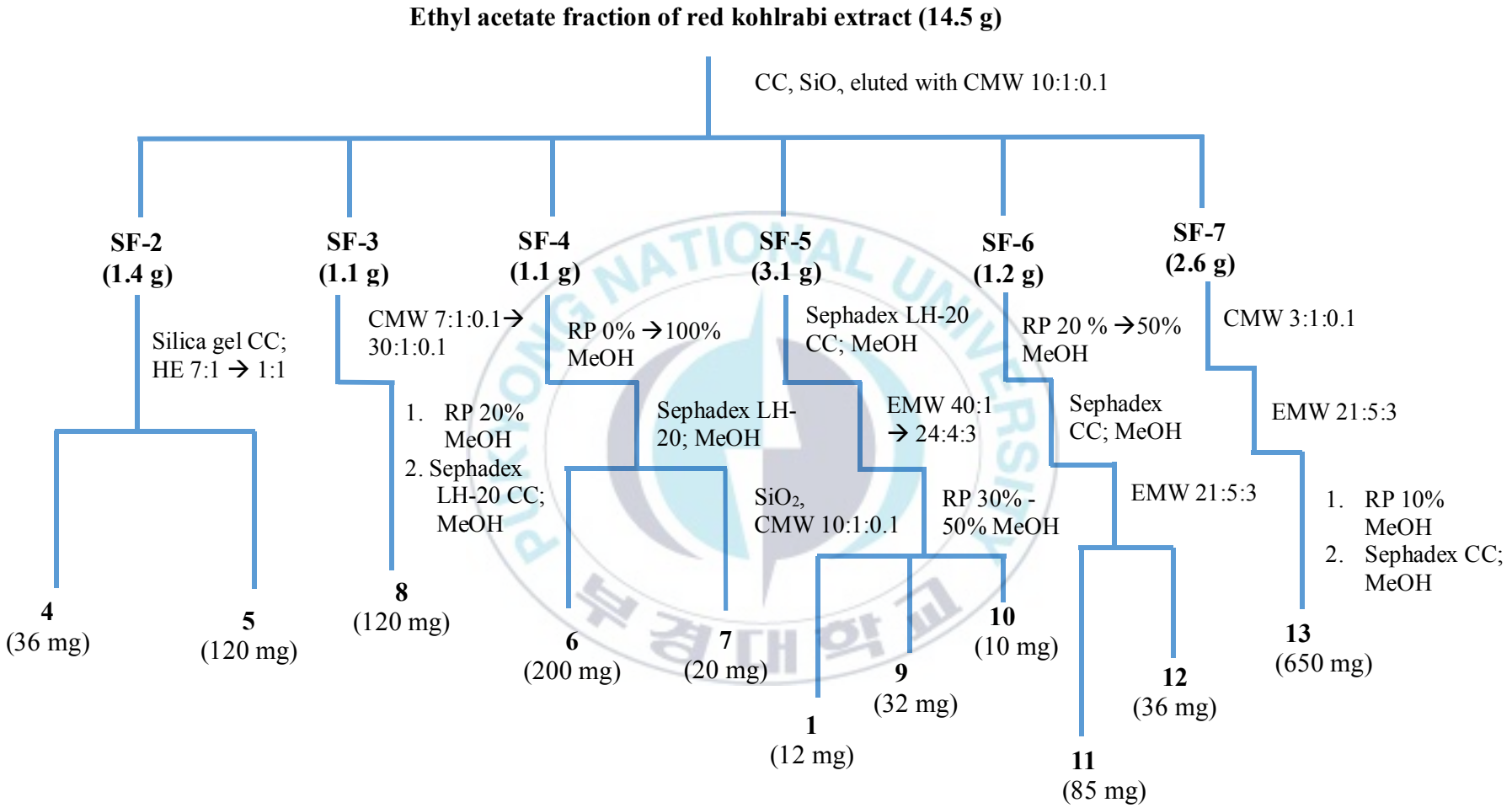

Scheme 2. Isolation of compounds from the EtOAc fraction *of B. oleracea* var. *gongylodes*.

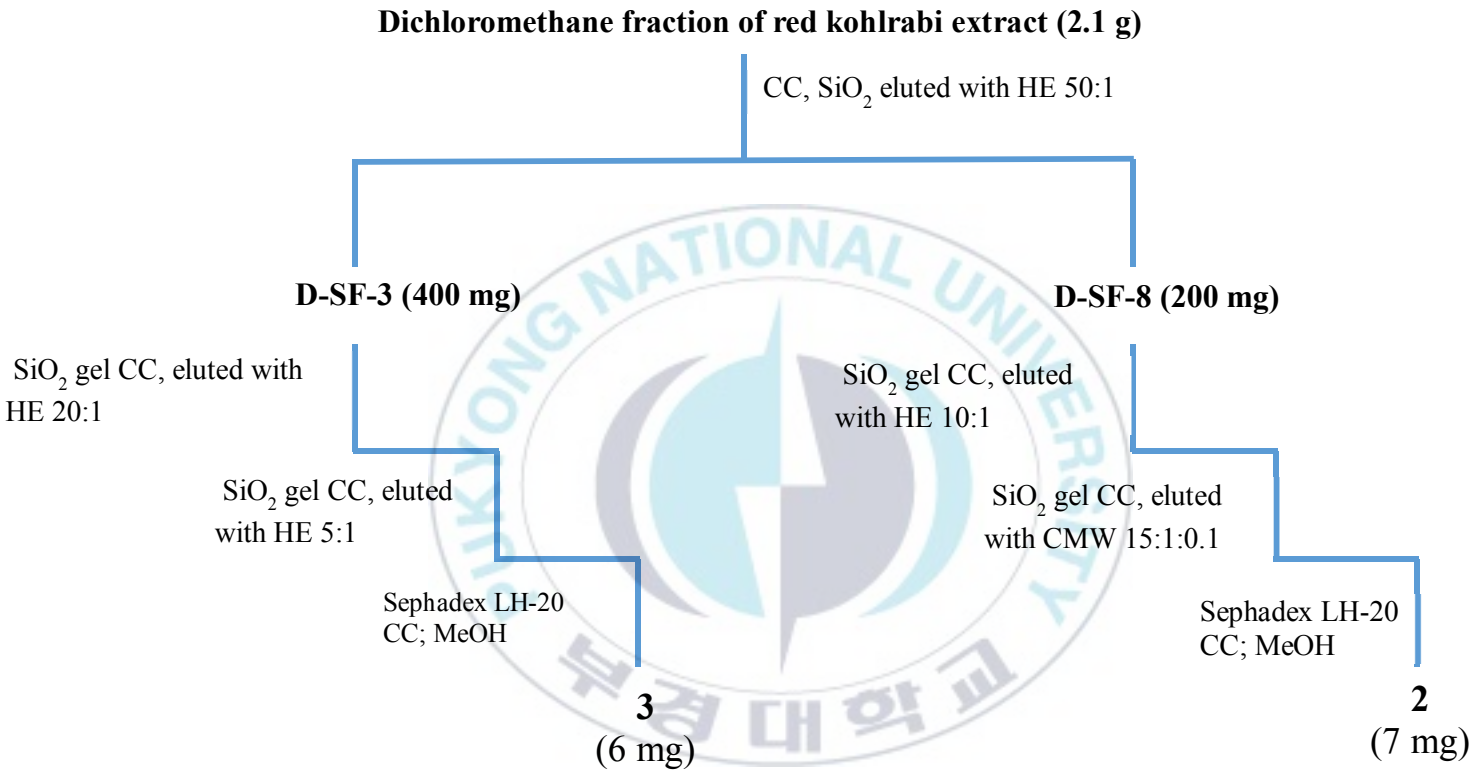

Scheme 3. Isolation of compounds from the CH_2Cl_2 fraction of *B. oleracea* var. *gongylodes*.

*1-methoxyindole 3-carboxylic acid 6-O- β-D-glucopyranoside (**1**)*. Brown semi-solid. **[α]$_D^{22.5}$** = - 5.28 ° (c 0.006, CH_3OH); **UV** (MeOH) λ_{max} (logε): 228 (4.70), 288 (4.23); **ESI-MS** *m/z*: 392.0953 $[M + Na]^+$ (calcd for $C_{16}H_{19}NNaO_9$, 392.0952); **IR** (KBr, ν_{max}, cm^{-1}): 808, 1034, 1221, 1325, 1517, 1675, 2850, 2922, 3341; **^{13}C NMR** and **^{1}H NMR** (Table 1).

*Indole 3-acetonitrile (**2**)*. **UV** (MeOH) λ_{max}: 216, 244, 295; **EI-MS** *m/z*: 156 $[M]^+$, 131, 101, 117, 101, 89, 77, 63; **^{13}C NMR** (600 MHz, CD_3OD) δ: 138.16 (C-7a), 127.48 (C-3a), 124.36 (C-2), 123.04 (C-6), 120.33 (C-5) 120.03 (C-10), 118.80 (C-4), 112.58 (C-7), 105.07 (C-3), 14.23 (C-9); **^{1}H NMR** (600 MHz, CD_3OD) δ: 7.57(1H, d, J = 8.3 Hz, H-4), 7.37 (1H, d, J = 8.3 Hz, H-7), 7.23 (1H, s, H-2), 7.15 (1H, t, J = 7.2 Hz, H-6), 7.07 (1H, t, J = 7.6 Hz, H-5), 3.93 (2H, s, H-9).

*N-methoxyindole 3-acetonitrile (**3**)*. **EI-MS** *m/z*: 186 $[M]^+$,171, 155, 146, 128, 116, 101, 77, 63; **ESI-MS** *m/z*: 209.0689 $[M + Na]^+$; **^{13}C NMR** (600 MHz, CD_3OD) δ:133.79 (C-7a), 124.08(C-7), 123.96 (C-3a), 123.15 (C-6), 121.27 (C-5), 119.58 (C-4), 119.50 (C-11), 109.46 (C-2), 102.12 (C-3), 66.48 (N-OCH_3), 14.03 (C-11); **^{1}H NMR** (600 MHz, CD_3OD) δ: 7.60 (1H, d, J = 7.6 Hz, H-4), 7.43 (1H, d, J = 10.3 Hz, H-7), 7.25 (1H, t, J = 8.3 Hz, 15.12 Hz, H-6), 7.13 (1H, dd, J = 1.38, 15.12 Hz, H-5), 7.12 (1H,s, H-2), 4.07 (3H, s, N-OCH_3), 3.933 (2H, s, H-10).

*β-Sitosterol glucoside (**4**)*. Brown powder. Confirmed by TLC comparison with reference compound.

*5-hydroxymethyl-2-furaldehyde (**5**)*. Yellow oil. **^{13}C NMR** (600 MHz, CD_3OD) δ: 179.43 (C-1), 163.19 (C-5), 153.89 (C-2), 124.83 (C-3), 110.89 (C-4), 57.53 (C-6); **^{1}H NMR** (600 MHz, CD_3OD) δ: 9.25 (1H, s, -CHO),

7.38 (1H, d, J = 3.5 Hz, H-3), 6.58 (1H, d, J = 4.1 Hz, H-4), 4.60 (2H, s, H-6).

*Methyl-1-thio-β-D-glucopyranosyl disulfide (**6**)*. Colorless gum. **EIMS** *m/z* 163, 145, 127, 85, 73, 61, 45; **ESI-MS** *m/z*: 265.0175 $[M + Na]^+$(calcd for $C_7H_{14}NaO_5S_2$, 265.175) ; **^{13}C NMR** (C_5D_5N, 600 MHz) δ: 93.064 (C-1), 73.359 (C-2), 80.569 (C-3), 71.856 (C-4), 83.642 (C-5), 63.382 (C-6), 25.083 (C-7); **^{1}H NMR** (C_5D_5N, 600 MHz) δ: 2.572 (3H, s, CH_3S), 5.079 (1H, d, J = 8.9 Hz, H-1), 4.008 (1H, m, H-2),4.365 (1H, d, J = 5.4 Hz, H-3), 4.343 (1H, d, J = 5.4 Hz, H-4), 4.298 (1H, q, J = 2.1 Hz, 2.8 Hz, 3.4Hz, 8.2 Hz, H-5), 4.567 (1H, dd, J = 2.7 Hz, 12 Hz, H-6a), 4.547(1H, dd, J = 2.1 Hz,12 Hz, H-6b).

*5-Hydroxy-2-pyridinemethanol (**7**)*. White crystal. **EIMS** *m/z*: 124, [M]+, 108, 96, 78, 68, 52, 41; **^{13}C NMR** (CH_3OD, 600 MHz) δ: 137.222 (C-1), 154.696 (C-2), 123.319 (C-3), 125.005 (C-4), 152.465 (C-5), 35.229 (C-6); **^{1}H NMR** (CH_3OD, 600 MHz) δ: 8.01 (1H, d, J = 3 Hz, H-6), 7.36 (1H, J = 9 Hz, H-3), 7.233 (1H dd, J = 3.6 Hz, 5.4 Hz, H-4), 4.579 (2H, s, H-7).

*(3S, 4R)-2-Deoxyribonolactone (**8**)*. Colorless semisolid. **$[\alpha]_D^{25}$** = + 0.128° (c 0.013, CH_3OH); **ESI-MS** *m/z*: 155.0318 $[M + Na]^+$ (calcd for $C_5H_8NaO_4$, 155.0135); **EIMS** *m/z*: 101, 83,57,43; **^{13}C NMR** (CH_3OD, 600 MHz) δ: 178.633 (C-1), 39.157 (C-2), 70.141 (C-3), 91.172 (C-4), 64.511 (C-5); **^{1}H NMR** (CH_3OD, 600 MHz) δ: 2.365 (1H, dd, J = 2.75 Hz, 17.85 Hz, H-2), 2.905 (1H, dd, J = 6.9Hz, 17.85 Hz, H-2), 3.752 (1H, dd, J = 4.1 Hz, 12.4 Hz, H-5), 3.681 (1H, dd, J = 2.8 Hz, 12.4 Hz, H-5), 4.358 (1H, q, J = 3.5 Hz, 2.7 Hz, 2.4 Hz, H-3), 4.418 (1H, m, H-4).

*n-Butyl-β-D-fructopyranoside (**9**)*. Amorphous white powder. **^{13}C NMR** (CD_3OD, 400 MHz) δ: 101.60 (C-2), 71.53 (C-4), 71.09 (C-5), 70.55 (C-3),

65.16 (C-6), 63.46 (C-1), 61.62 (C-1'), 33.32 (C-2'), 20.51 (C-3'), 14.33 (C-4'); **^{1}H NMR** (CD_3OD, 400 MHz) δ: 3.90 (1H, d, J = 9.6 Hz, H-3), 3.82 (1H, q, H-5), 3.77 (1H, dd, J = 4.6, 3.2 Hz, H-4), 3.74 (1H, dd, J = 4.2, 2.1 Hz, H-6a), 3.73 (1H, d, J = 4.1 Hz, H-1a), 3.69 (1H, d, J = 11.6 Hz, H-1b), 3.64 (1H, dd, J = 12, 1.4, H-6b), 3.49 (2H, td, J = 9.2, 6.8 Hz, H-1'), 1.56 (2H, m, H-2'), 1.40 (2H, m, H-3') , 0.99 (3H, t, H-4').

*Uridine (**10**)*. White crystal. **EIMS** *m/z*: 155, 141, 127, 113, 111, 98, 85,71, 57, 43; **^{13}C NMR** (CD_3OD, 600 MHz) δ: 157.128 (C-2), 172.735 (C-4), 103.011 (C-5), 141.837 (C-6), 91.464 (C-1'), 75.790 (C-2'), 71.242(C-3'), 86.045 (C-4'), 62.386(C-5'); **^{1}H NMR** (CD_3OD, 600 MHz) δ: 7.699 (1H, d, J = 7.8 Hz, H-6), 5.877 (1H, d, J = 4.8 Hz, H-1'), 5.663 (1H, d, J = 7.2, H-5), 4.163 (1H, t, J = 4.8, 9.6 Hz, C-3'), 4.134(1H, t, J = 4.8, 10.2 Hz, H-2'), 3.965 (1H, m, H-4'), 3.828 (1H, dd, J = 2.4, 12.3 Hz, H-5'), 3.718 (1H, dd, J = 3.6, 14.4 Hz, H-5').

Tagatose (11). Colorless syrup. **EIMS** *m/z*: 119, 103, 86, 73, 60, 43; Confirmed by TLC comparison with compounds **12** and **13**, and EIMS library search.

*β-D-Fructofuranose (**12**)*. Colorless syrup. **^{13}C NMR** (CH_3OD, 600 MHz) δ: 61.514 (C-1), 105.204 (C-2), 78.730 (C-3), 77.198 (C-4), 83.488 (C-5), 64.712 (C-6); **^{1}H NMR** (CH_3OD, 600 MHz) δ**:** 4.908 (1H, d, J = 8.3 Hz, H-3), 3.928 (1H, t, J = 15.1, 7.5 Hz, H-4), 3.729 (1H, m, H-5), 3.696 (1H, s, H-1), 3.6362 (1H, s, H-1), 3.577 (1H, dd, J = 6.8, 11.6, H-6), 3.528 (1H, dd, J = 6.6, 11.3 Hz, H-6).

*β-D-Fructopyranose (**13**)*. Viscous light yellow syrup. Confirmed by comparing TLC with reference.

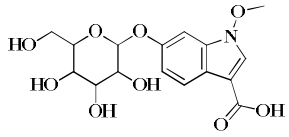

1-Methoxyindole 3-carboxylic acid 6-*O*- β-D-glucopyranoside (**1**)

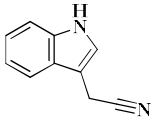

Indole 3-acetonitrile (**2**)

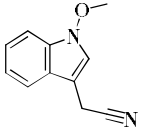

N-methoxyindole 3-acetonitrile (**3**)

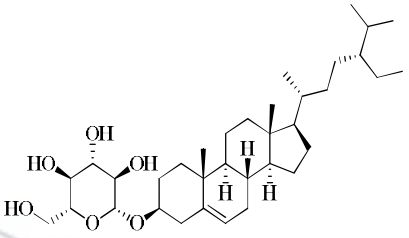

β-Sitosterol glucoside (**4**)

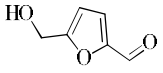

5-Hydroxymethyl-2-furaldehyde (**5**)

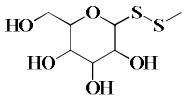

Methyl-1-thio-β-D-glucopyranosyl disulfide (**6**)

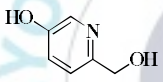

5-Hydroxy-2-pyridinemethanol (**7**)

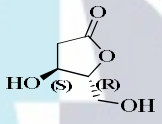

(3S, 4R)-2-Deoxyribolactone (**8**)

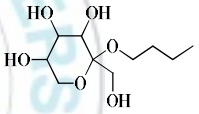

n-Butyl-β-D-fructopyranoside (**9**)

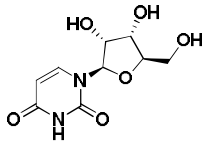

Uridine (**10**)

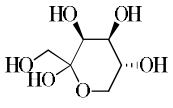

Tagatose (**11**)

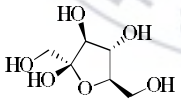

β-D-Fructofuranose (**12**)

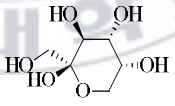

β-D-Fructopyranose (**13**)

Figure 1. Structures of compounds isolated from *Brassica oleracea* var. *gongylodes*.

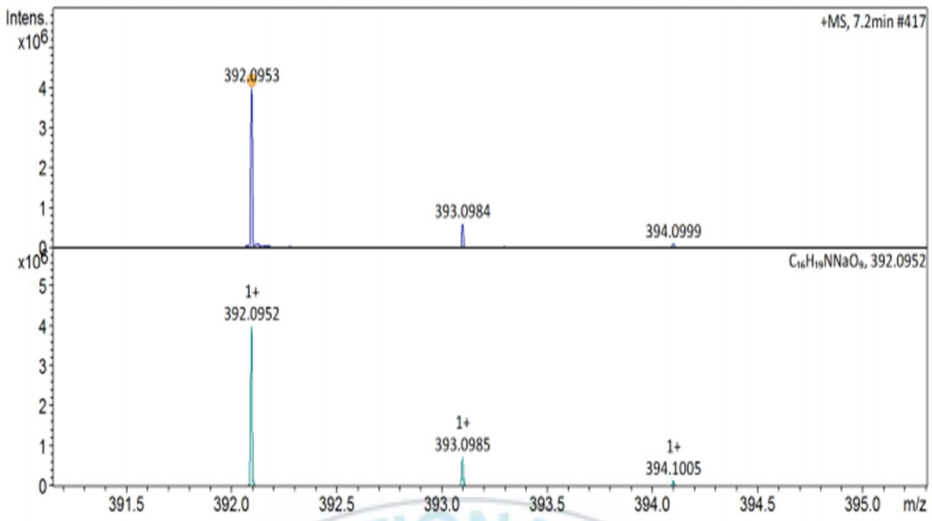

Figure 2. HR-ESIMS spectrum of compound **1.**

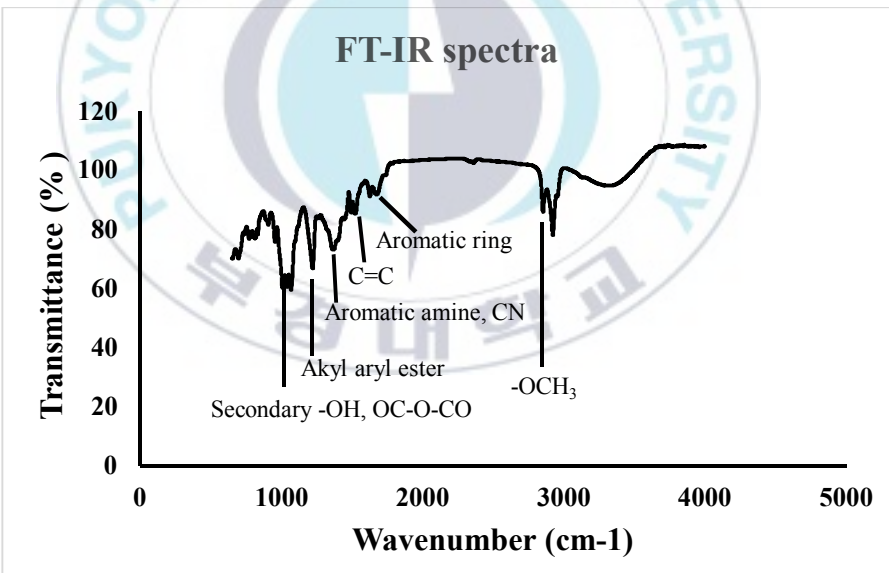

Figure 3. FT-IR spectrum of compound **1.**

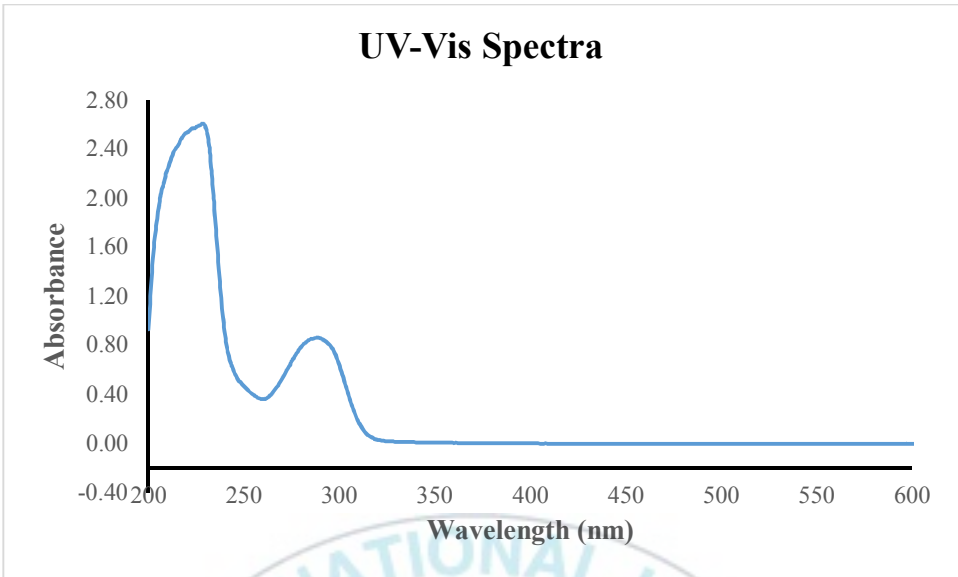

Figure 4. UV-Vis spectrum of compound **1.**

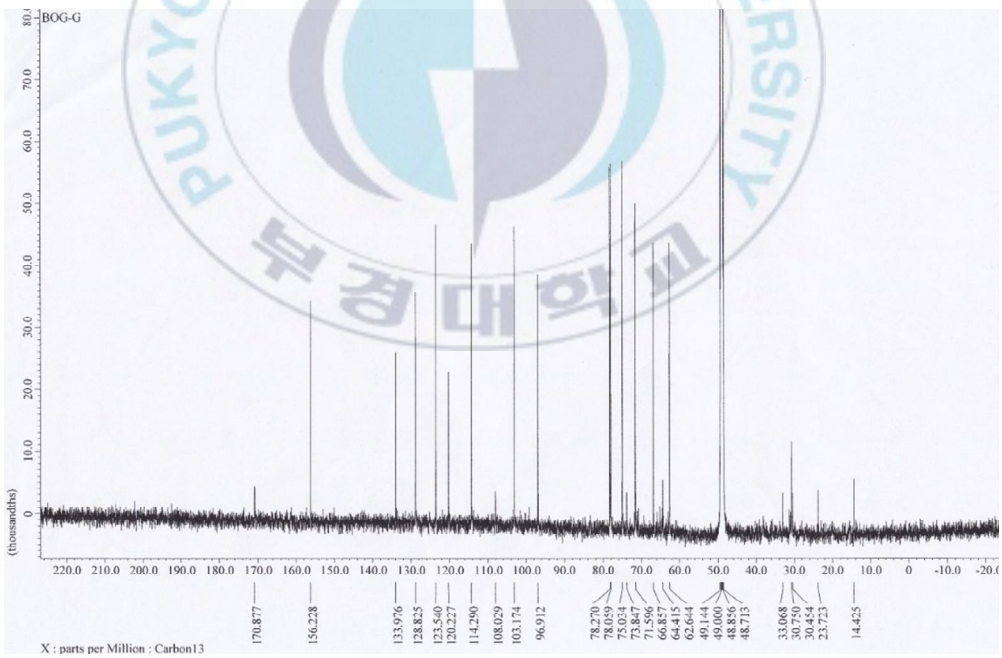

Figure 5. ^{13}C NMR spectrum of compound **1.**

Figure 6. ^{1}H NMR spectrum of compound **1**.

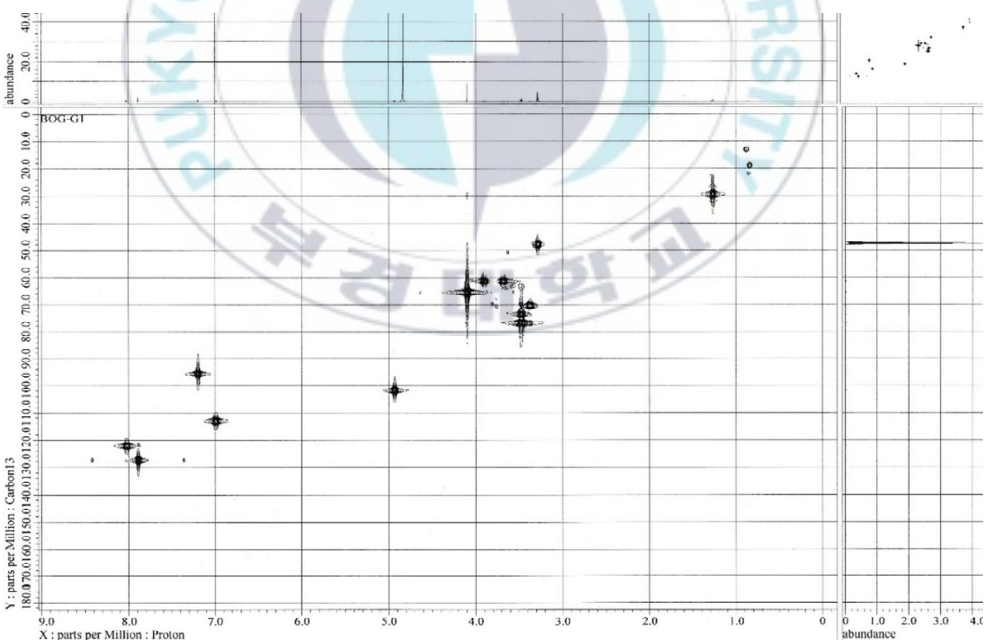

Figure 7. HMQC spectrum of compound **1**.

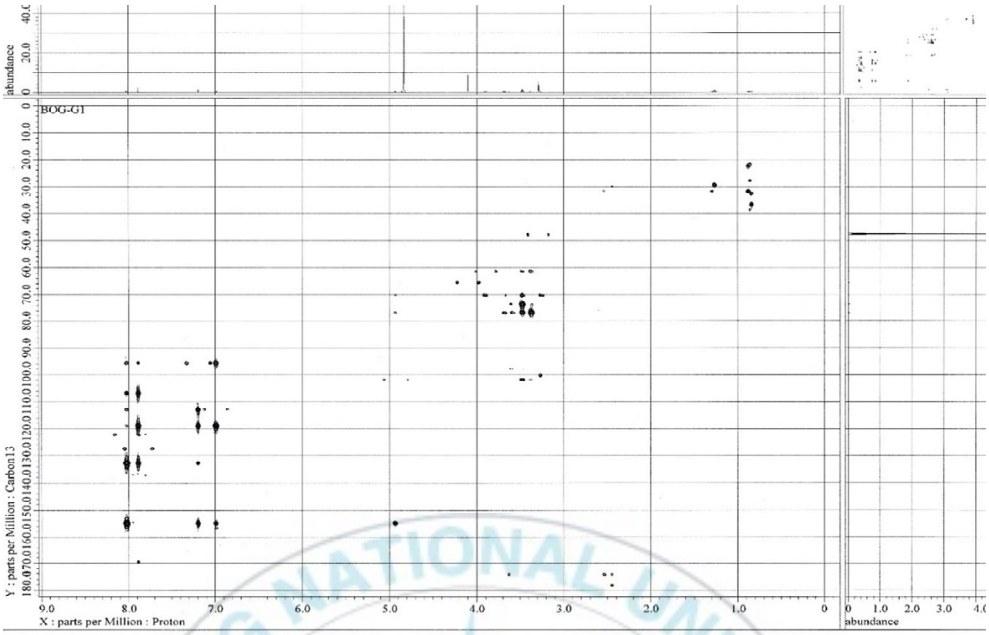

Figure 8. HMBC spectrum of compound **1**.

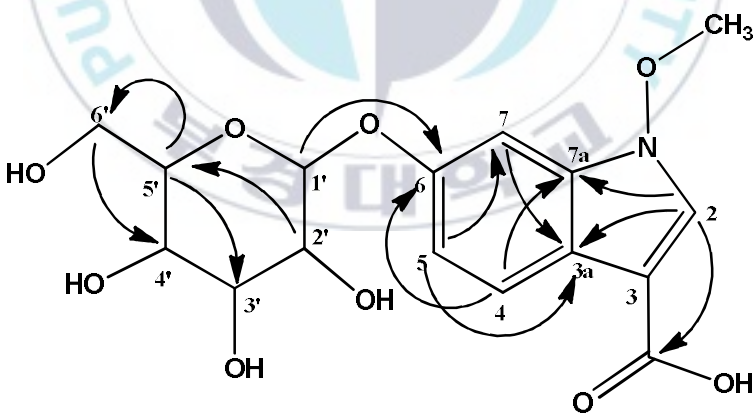

Figure 9. HMBC correlations in the structure of compound **1**.

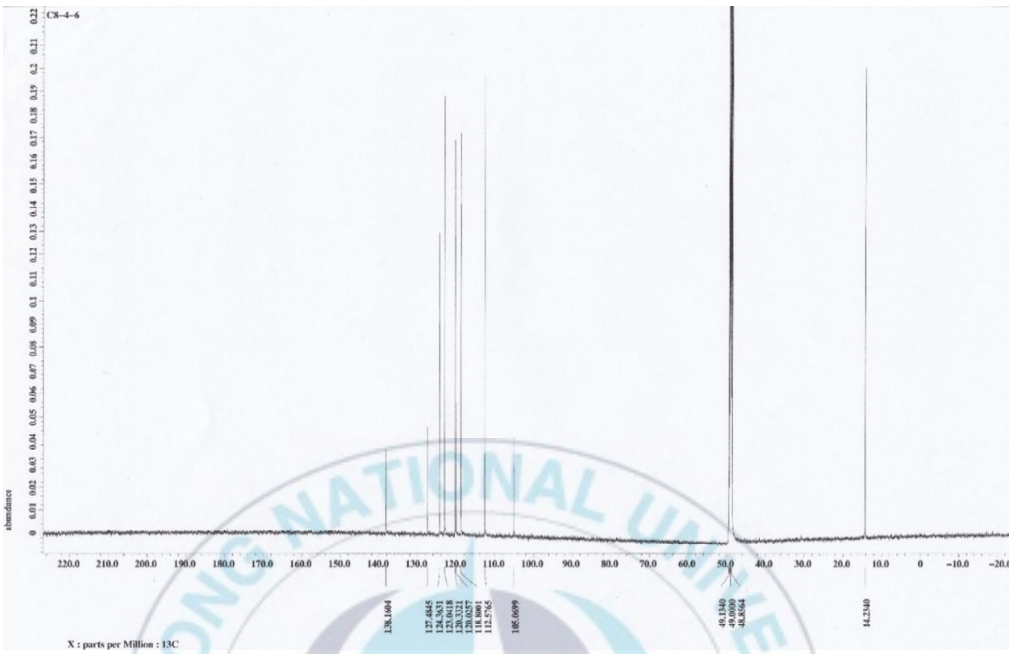

Figure 10. ^{13}C NMR spectrum of compound **2**.

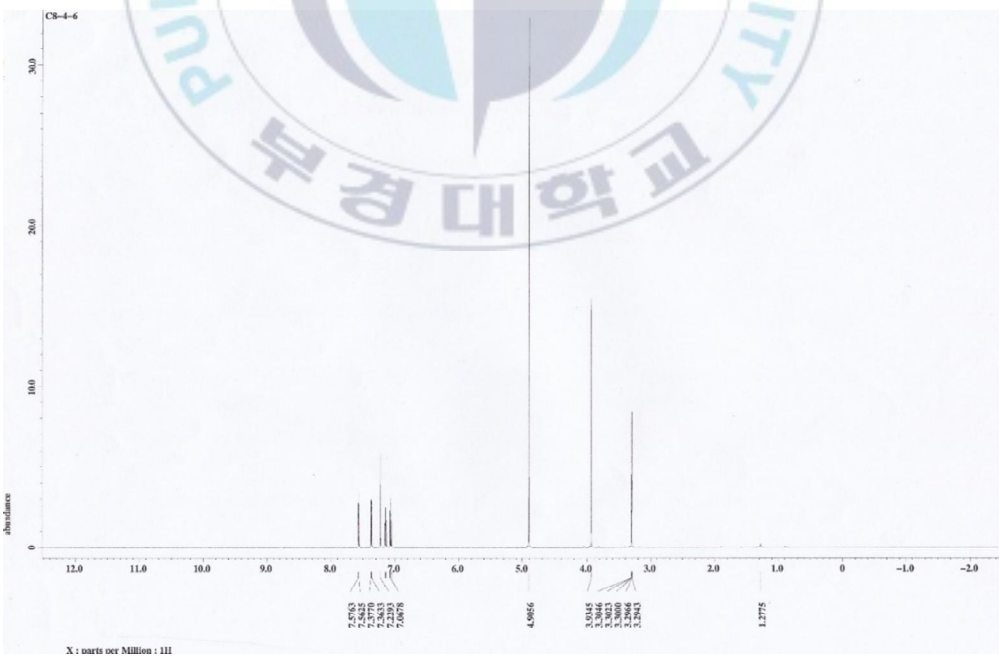

Figure 11. ^{1}H NMR spectrum of compound **2**.

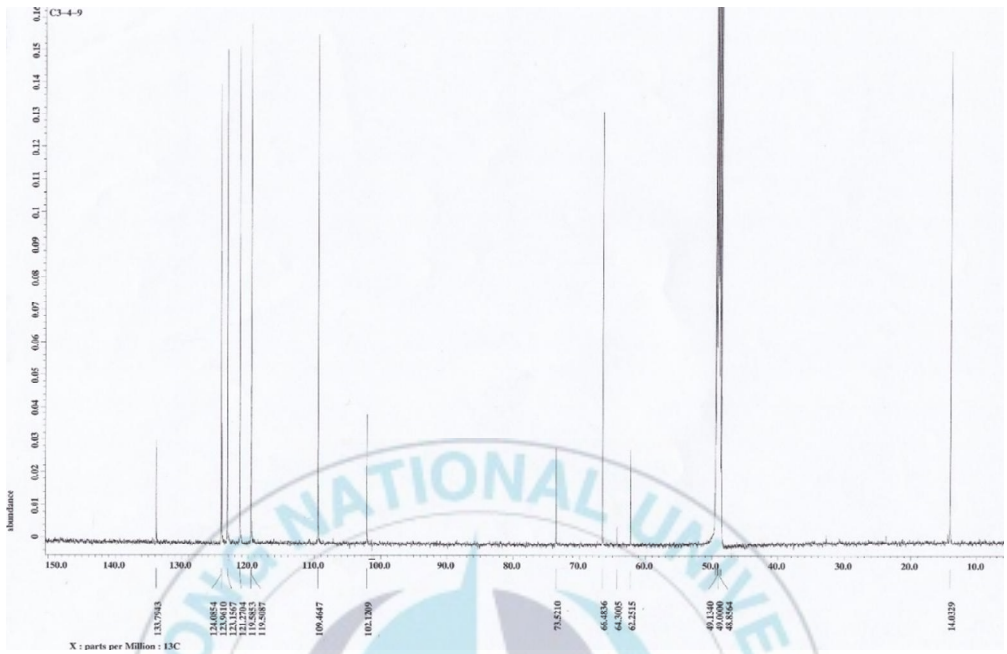

Figure 12. ^{13}C NMR spectrum of compound **3**.

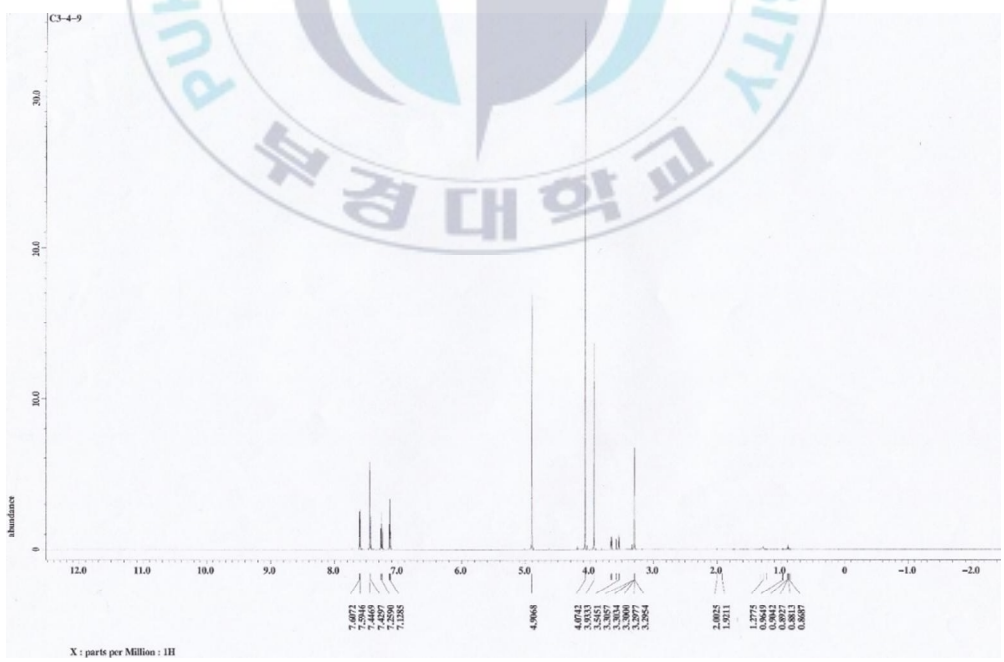

Figure 13. ^{1}H NMR spectrum of compound **3**.

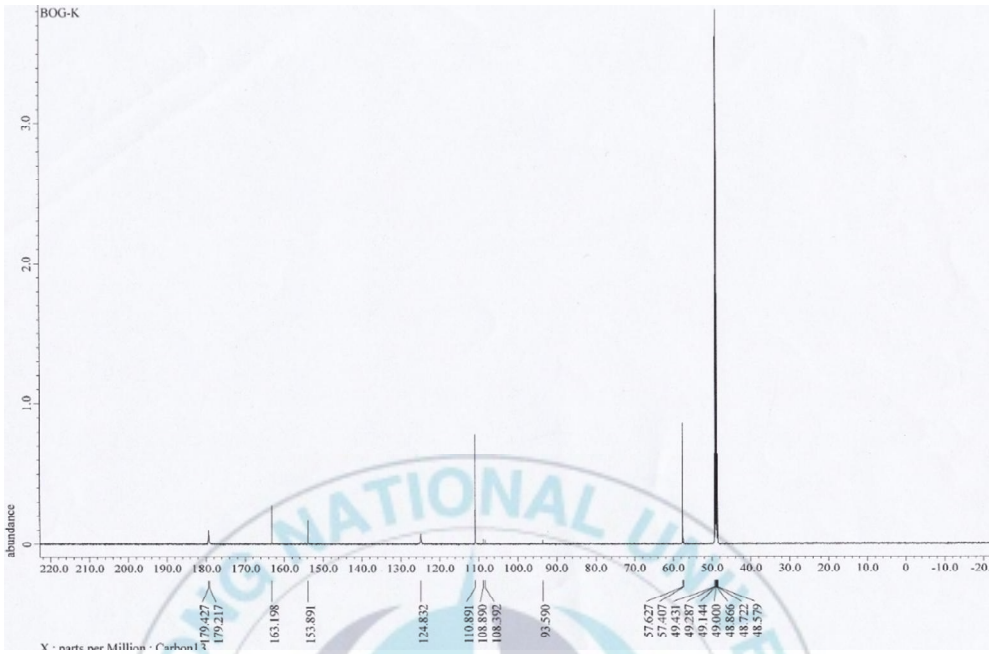

Figure 14. ^{13}C NMR spectrum of compound **5**.

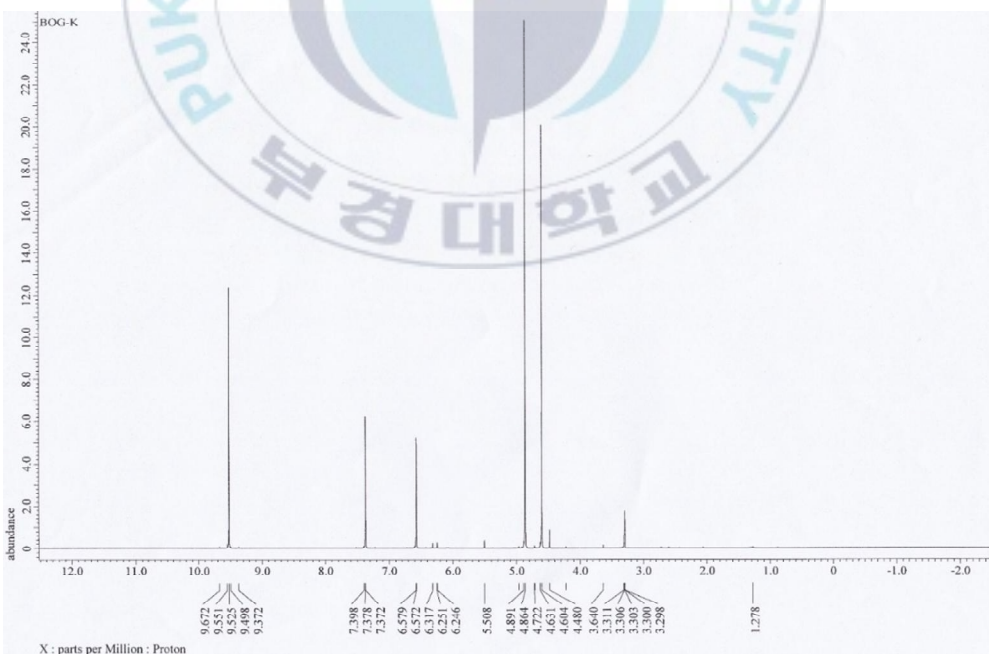

Figure 15. ^{1}H NMR spectrum of compound **5**.

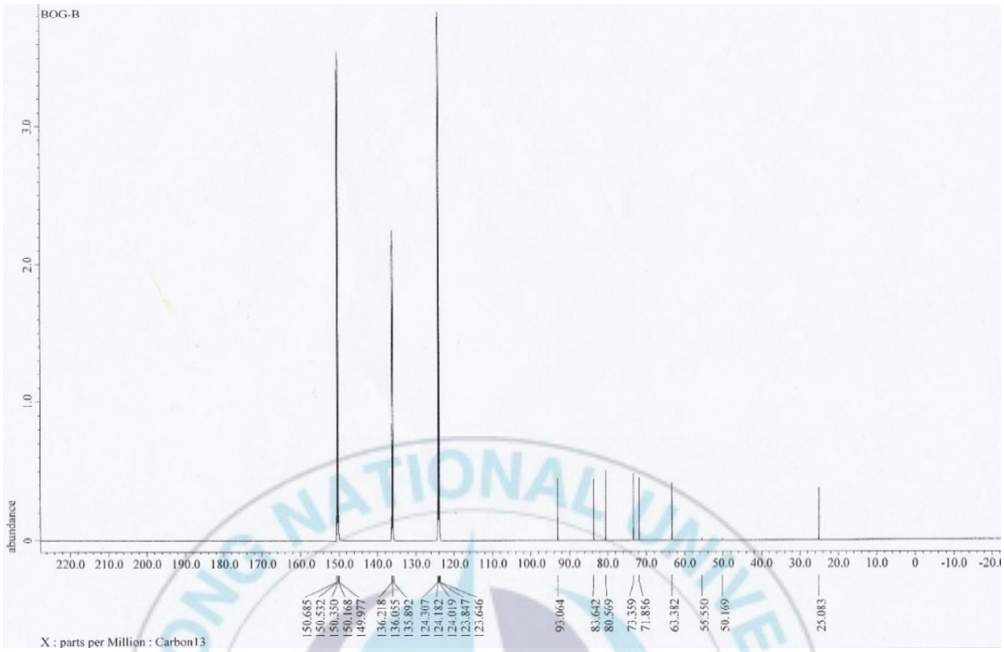

Figure 16. ^{13}C NMR spectrum of compound **6**.

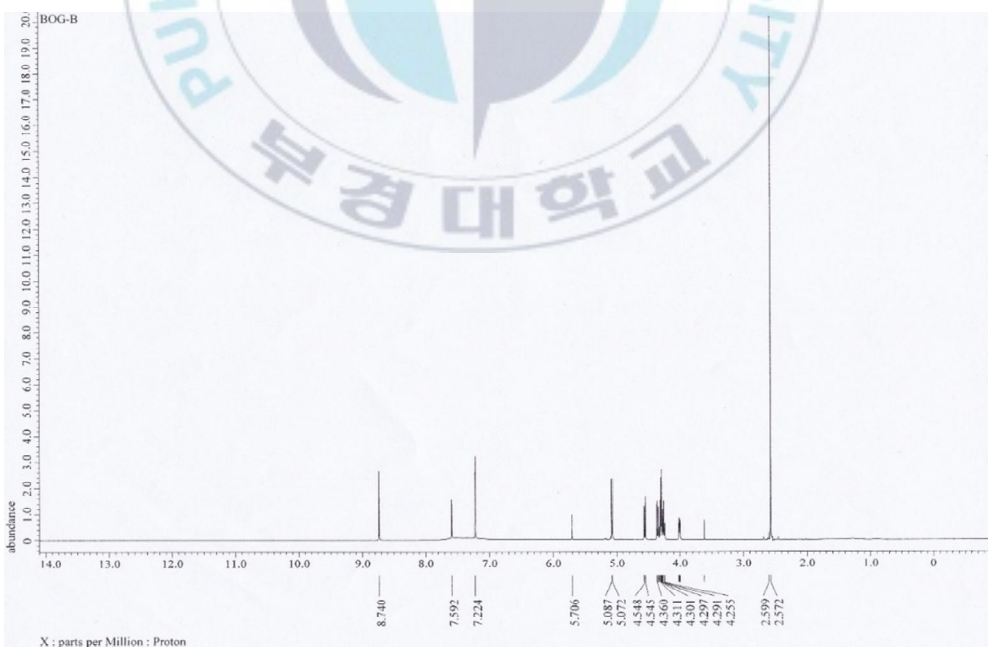

Figure 17. ^{1}H NMR spectrum of compound **6**.

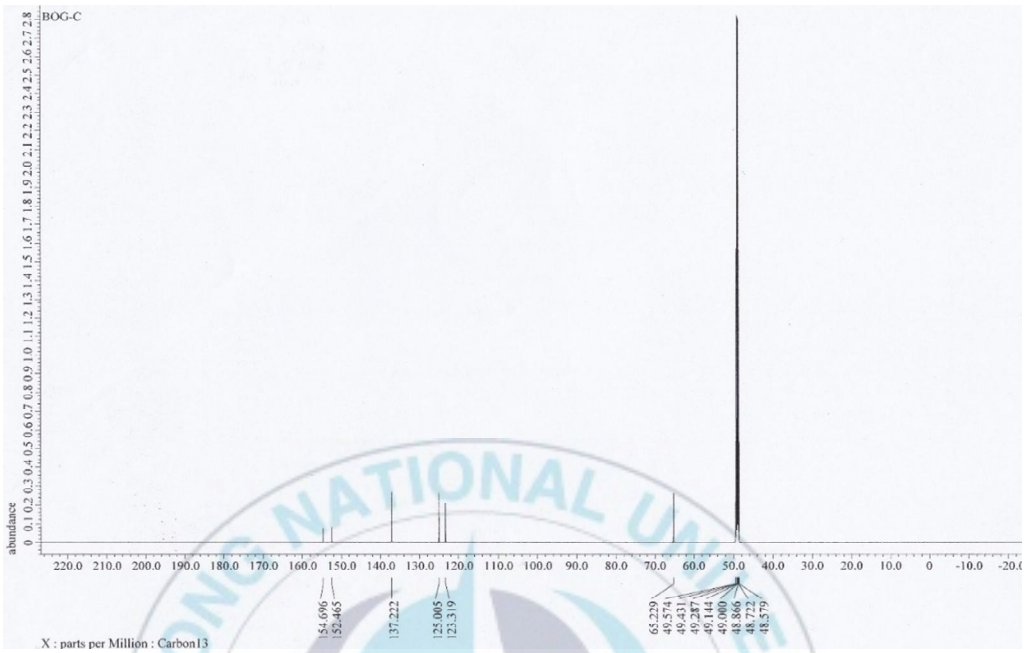

Figure 18. ^{13}C NMR spectrum of compound **7**.

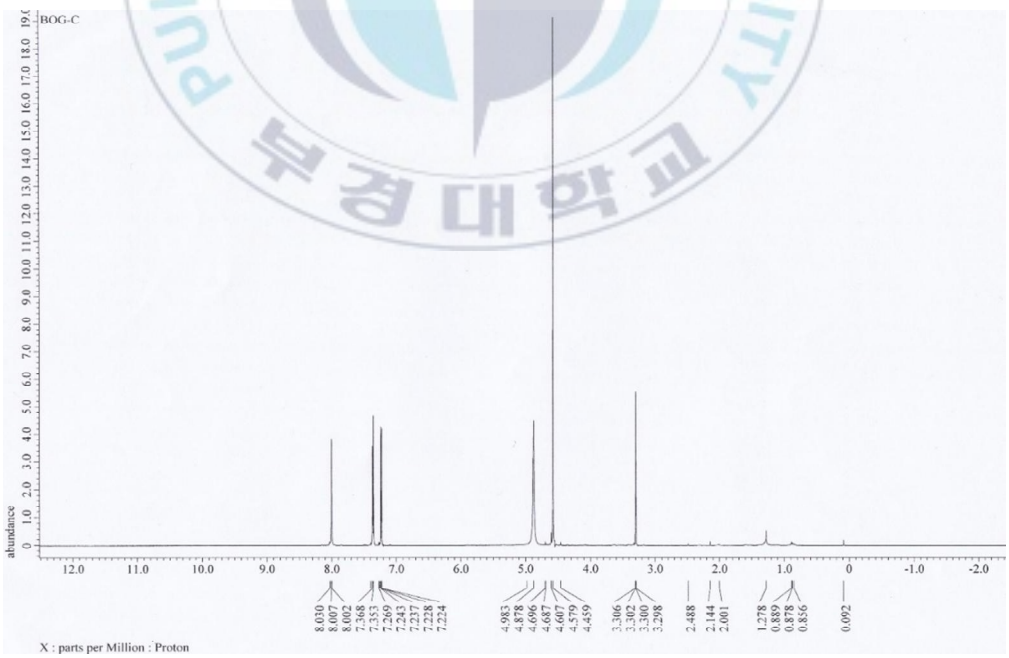

Figure 19. ^{1}H NMR spectrum of compound **7**.

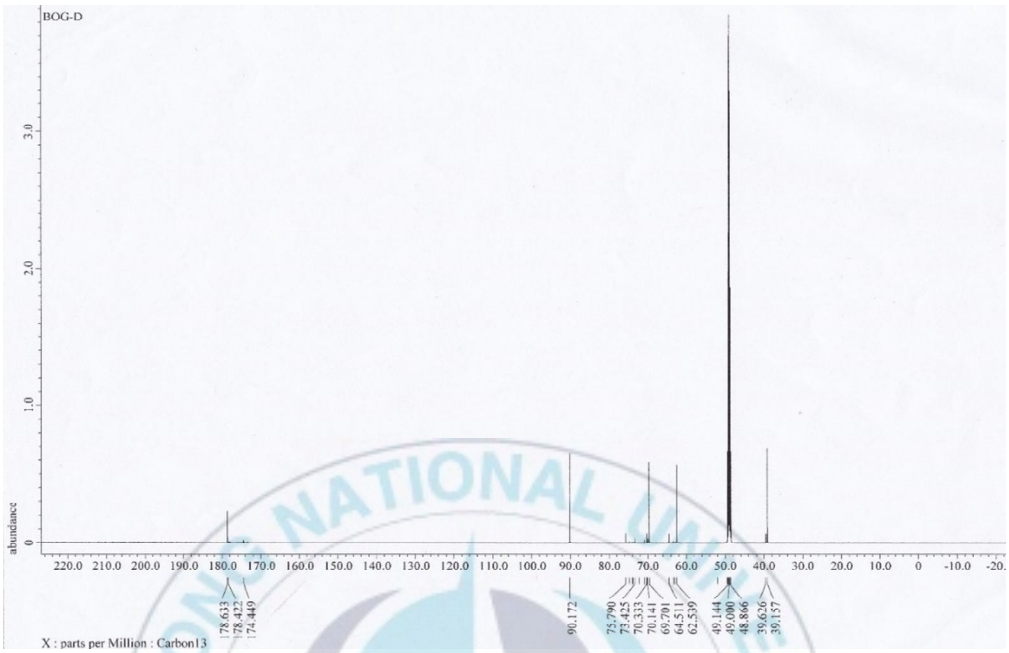

Figure 20. ^{13}C NMR spectrum of compound **8**.

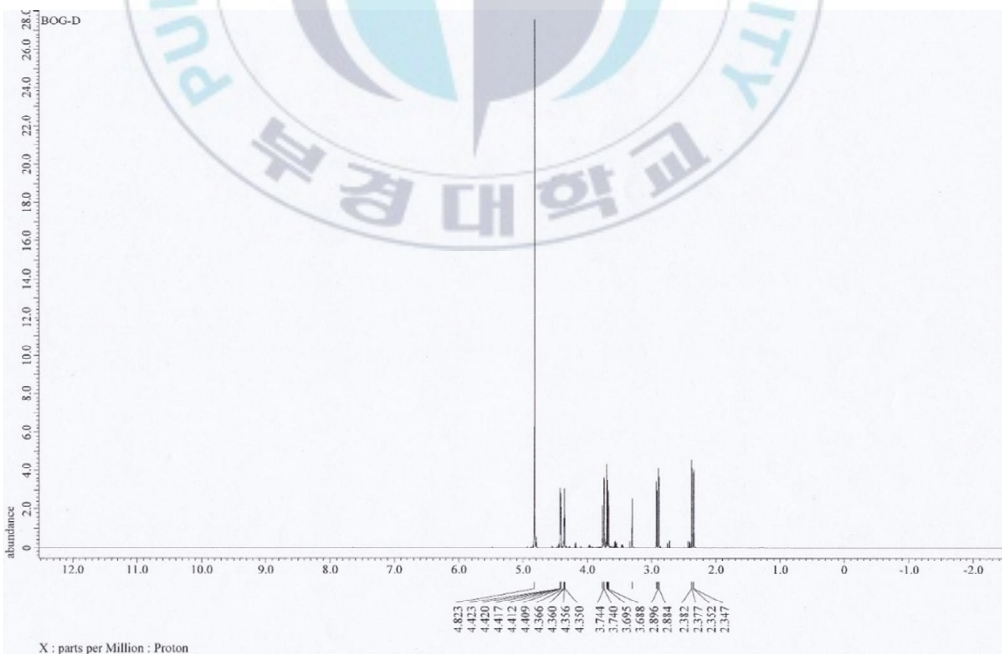

Figure 21. ^{1}H NMR spectrum of compound **8**.

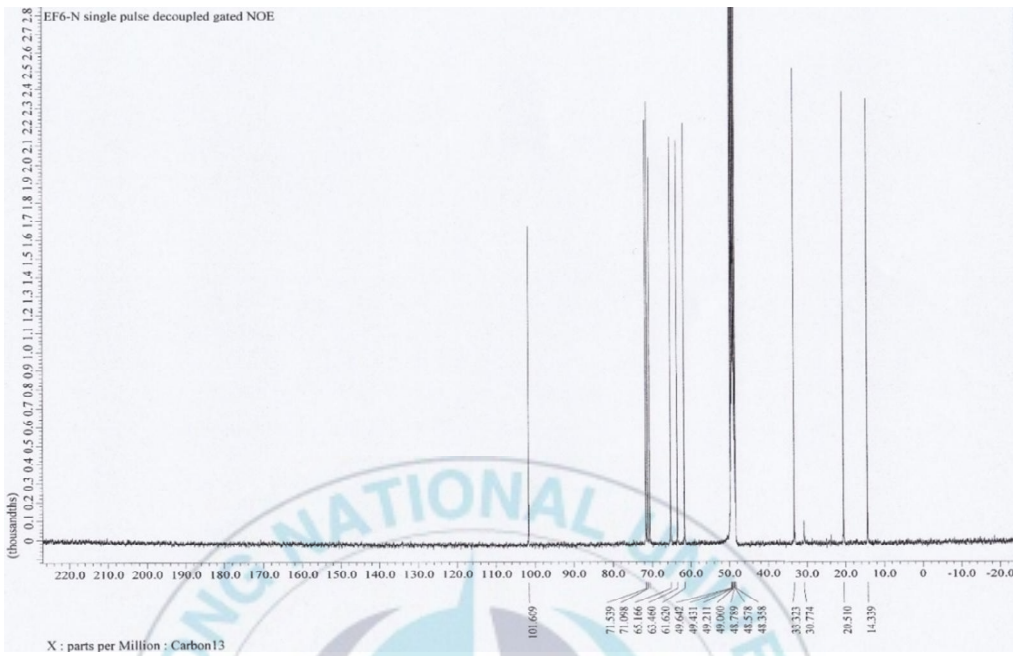

Figure 22. ^{13}C NMR spectrum of compound **9**.

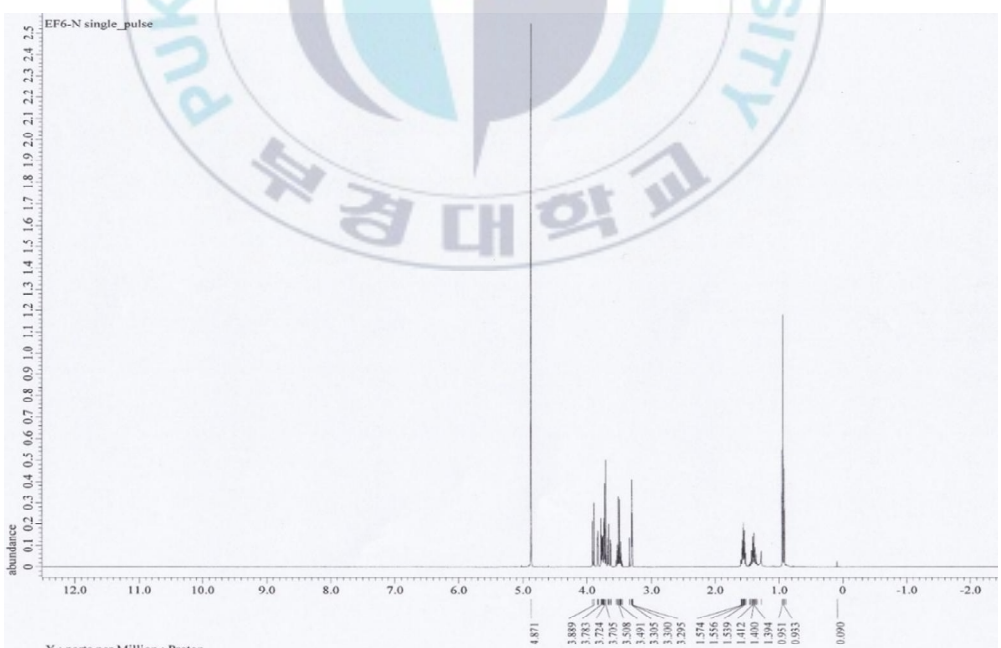

Figure 23. ^{1}H NMR spectrum of compound **9**.

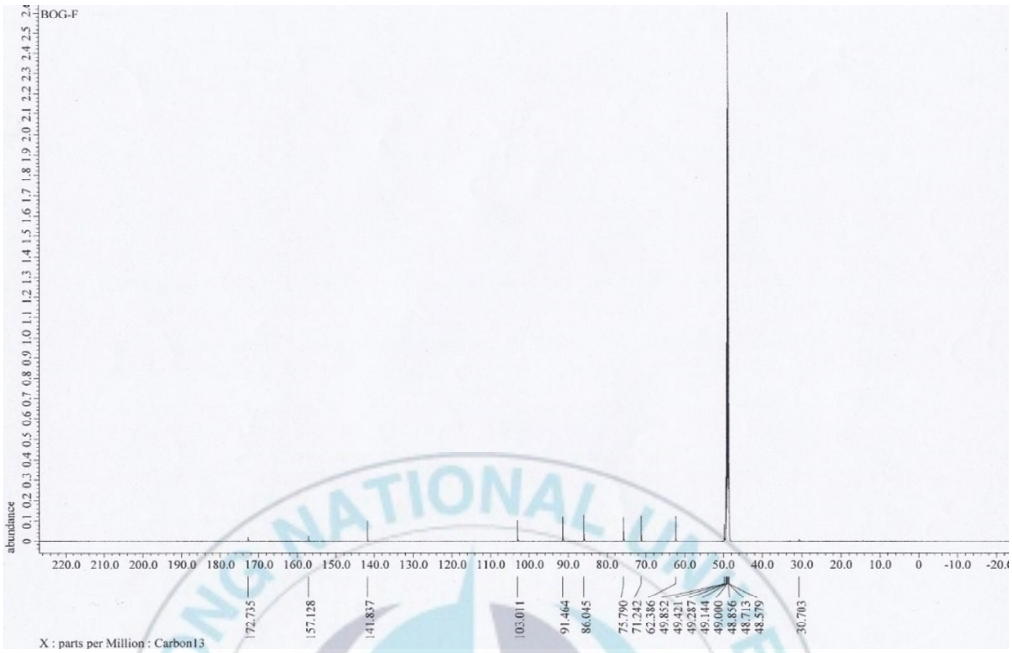

Figure 24. ^{13}C NMR spectrum of compound **10**.

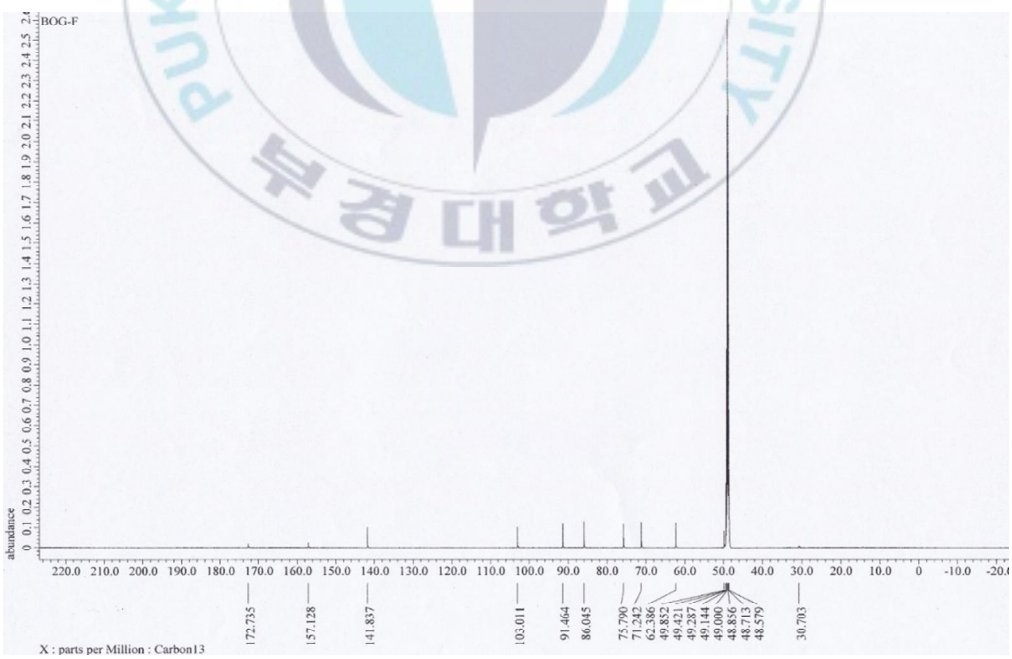

Figure 25. ^{1}H NMR spectrum of compound **10**.

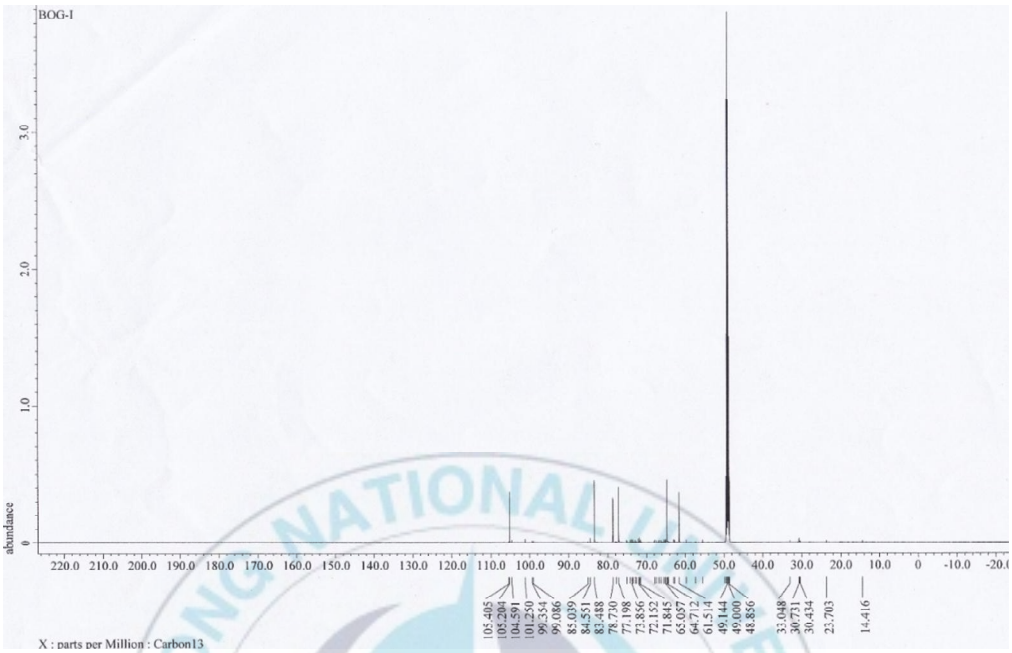

Figure 26. ^{13}C NMR spectrum of compound **12**.

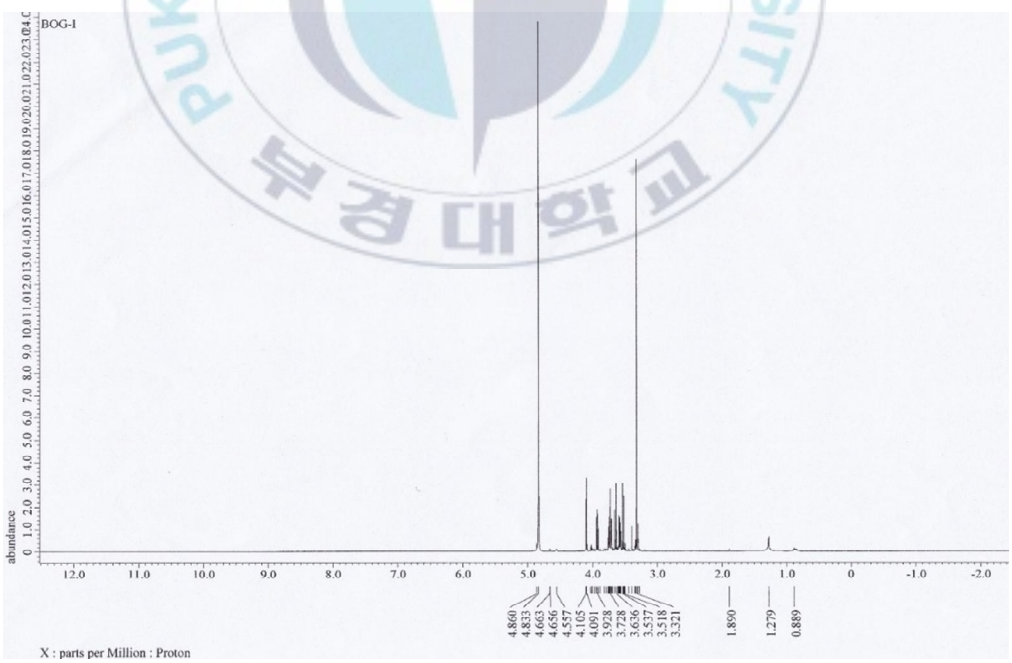

Figure 27. ^{1}H NMR spectrum of compound **12**.

3. Results

3.1 Structure elucidation of compound 1

Compound **1** was obtained as brown solid, soluble in methanol. The HR-ESI-MS gave a pseudomolecular ion peak at *m/z* 392.0953 $[M+Na]^+$, corresponding to an elemental formula of $C_{16}H_{19}NNaO_9$, *m/z* 392.0952, with eight degree of unsaturation (Figure 2). It showed UV spectrum with λ_{max} (logε) at 228 (4.70) and 288 (4.23), suggesting the indole-related compound (Yang et al., 2014). Optical rotation was measured as $[\alpha]_D^{22.5}$ = - 5.28 ° (c 0.006, CH_3OH). IR spectrum revealed the presence of O-methoxy (2850 cm^{-1}), C=C stretching (1517 cm^{-1}), aromatic ring (1675 cm^{-1}), aromatic amine –CN stretching (1325 cm^{-1}), aryl alkyl ester (1221 cm^{-1}) and secondary cyclic alcohol (1005-1069 cm^{-1}).

^1H NMR spectrum of compound **1** exhibited signals for four aromatic protons (7.903, s; 8.037, d, J=8.9 Hz; 7.005, dd, J= 8.5,2 Hz and 7.210, d, 2.1 Hz) assigned to H-2, H-4, H-7 and H-5; and one N-methoxy group (δ_H 4.113, s). While ^{13}C NMR spectrum (Table 1) showed the presence of four quaternary carbons (156.28, 133.97, 120.22, 108.02), one CH_2 (62.64), nine CH groups and one carbonyl carbon (170.87). In addition, ^1H and ^{13}C NMR data presented the signals attributable to a glucose moiety. The spectrum confirmed the existence of an indolyl moiety and a glucopyranosyl in **1**. Further, ^1H and ^{13}C signals closely resembled with 6-hydroxyindole-3-carboxylic acid 6-O-β-D-glucopyranoside (Bednarek et al., 2005; Montaut and Bleeker, 2010) except for the addition of methoxy group in the indole ring at N-position which changes the chemical shift in the pyrrole moiety of indole ring. This was established by HMBC and HMQC data.

Furthermore, the NMR signals of aglycone moiety are similar to those of 1-methoxyindole-3-carboxylic acid (Somei et al., 2001; Yang et al., 2014). HMBC spectrum showed correlations between anomeric proton at δ 4.936 (1H, dd, J= 7.6, 2.4 Hz) and C-6 (156.22), indicating β-configuration of glucopyranosyl moiety. The HMBC spectroscopic data revealed correlation of H-2 with δ_C 170.88 and 108.02, confirming the presence of –COOH group in C-3 position. The HMQC showed cross-peak of δ_H 4.11 (3H, s) with δ_C 66.85 having no correlations with other carbons and hydrogen indicating the presence of methoxy group in N-position. Thus, compound **1** was determined as N-methoxy-6-hydroxyindole-3-carboxylic acid-6-O-β- D-glucopyranoside.

Table 1. ^{1}H and ^{13}C NMR (CD_3OD, 600 MHz) data with HMBC correlations.

Position	δH	δC	HMBC
N-methoxy-indole-3-carboxylate			
N-O-CH_3	4.113 (3H, s)	66.857	
2	7.903 (1H, s)	128.825	133.976, 120.277, 108.029, 96.912, 170.877
3		108.029	
3a		120.227	
4	8.0365 (1H, d, J = 8.9 Hz)	123.540	156.228, 133.976, 96.912, 108.029, 114.290, 120.227
5	7.005 (1 H; dd ; J = 8.5, 2 Hz)	114.290	120.277, 96.912, 156.228
6		156.228	
7	7.2104 (1H, d, J = 2.1 Hz)	96.912	114.290, 120.227, 156.228, 133.976
7a		133.976	
3-COOH		170.877	
Glucopyranoside			
1'	4.9535 (1H, dd, J = 7.6, 2.4 Hz)	103.174	156.228, 78.270, 71.596
2'	3.3722 (m)	78.270	78.059, 62.644, 75.034
3'	3.4664 (m)	75.034	103.174, 78.270, 156.228
4'	3.4878 (m)	78.059	71.596, 103.174, 156.228
5'	3.3905 (m)	71.596	78.270. 62.644
6'	3.9175 (1H, dd, J = 12, 2.4 Hz) 3.6985 (1H, dd, J = 6, 2.4 Hz)	62.644	71.596, 78.027

3.2 Structure elucidation of compound 2

Compound **2** was obtained as white solid. The EIMS showed a molecular ion peak at *m/z* 156.05 $[M]^+$, with fragmentation peaks at *m/z* 131 (CN), 117 (-NH) and 77 (C_6H_6).The proton and carbon chemical shifts resembled to that of 2-(1*H*-indol-3-yl) acetonitrile/ 3-indoleacetonitrile, reported by Morales-Rios and Nathan (1987) and Kim et al. (2004). The structure was confirmed by HMQC and HMBC correlations. The ^{1}H NMR showed the signals at chemical shifts related to aromatic ring (7.57, d, J = 8.3 Hz; 7.37, d, J = 8.3 Hz; 7.23, s; 7.15, t, J = 7.2 Hz; and 7.07, t, J = 7.6 Hz). The proton and carbon NMR indicated the presence of one $–CH_2$ group (δ_c 14.23 and δ_H 3.93, 2H, s) strongly correlated with δ_c 105.07, 120.33 and 124.36. HMQC showed the presence of three quaternary carbons (105.07, 120.33, 127.48 and 138.16), which were indicated as weak peaks in ^{1}H NMR (Kim et al., 2004; Morales□Ríos and Joseph□Nathan, 1987). The UV spectra showed the maximum absorption (λ_{max}) at 216, 244 and 295 nm indicating the presence of indole skeleton and an additional unsaturated bond (C≡ N).

3.3 Structure elucidation of compound 3

Compound **3** exhibited similar chemical shifts in ^{13}C NMR as of compound **2**, however an additional signal at δ_c 66.48 was observed. ^{1}H NMR consisted of a singlet peak at δ_H 4.07 with an integration of 3H, directing the presence of N-OCH_3 group as in compound **1**. This was established by the HMBC spectrum, which showed no correlation of its protons with the meta-carbons. As observed with compound **2**, a singlet signal at δ_H 3.93 (s, 2H) indicated the presence of $–CH_2$ group attached with aromatic carbon at C-3 (102.12), validated by HMBC correlation. EIMS analysis further

corroborated the existence of –OCH_3 group, shown by fragmentation peaks at 186, 171 and 155. Likewise the presence of –CN group can be predicted by difference in fragmentation patterns at m/z 155 and 128. ESIMS provided the molecular mass of the compound with molecular ion peak at m/z 290.0689, referring the elemental formula of $C_{11}H_{10}N_2ONa$. The compound was subsequently identified as N-methoxy indole-3-acetonitrile/ caulilexin C by comparing with reported spectral information (Bang et al., 2008; Pedras et al., 2006).

3.4 Structure elucidation of compound 5

Compound **5** was isolated as yellow oil. A single proton NMR peak was observed at δ_H 9.25 (1H, s) which denotes the aldehyde group in the molecule. Downfield proton peak at δ_H 4.60 (2H, s) suggested the presence of methylene adjacent to a hydroxyl group. Two downfield duplet peaks at δ_H 7.38 (1H, d, J = 3.5 Hz) and 6.58 (1H, d, J = 4.1 Hz) in ^{1}H NMR along with presence of four aromatic carbons at δ_C 110.89, 124.83, 153.89 and 163.19 ppm in ^{13}C NMR signified a 2, 5 disubstituted furfural ring system. ^{13}C NMR showed signals for an aldehyde carbon at δ_C 179.43 (C-1) and a methylene carbon at δ_C 57.53 (C-6) ppm. These results were consistent to that obtained for 5-hydroxymethyl-2-furaldehyde, reported by Kulkarni et al., 2008 and Luo et al., 2008, thus the compound **5** was determined to be 5-hydroxymethyl-2-furaldehyde (Kulkarni et al., 2008; Luo et al., 2009).

3.5 Structure elucidation of compound 6

Compound **6** occurred as colorless gum and consisted of signals relatable with glucoside moiety with seven carbon peaks and eight non-equivalent hydrogen peaks in ^{13}C and ^{1}H NMR spectrum respectively. ^{1}H NMR

spectrum revealed signals for –SCH_3 group (δ_H 2.57, 3H, s) corresponding to C-7 (δ_C 25.08), four oxygenated sp2 methine protons occurring in cyclic structure (δ_H 4.008, m, H-2; 4.365, d, J = 5.4, H-3; 4.343, d, J = 5.4 Hz, H-4; 4.298, q, J = 2.1 Hz, 2.8, 8.2 Hz, H-5), two methylene protons (δ_H 4.56, dd, J = 2.7 Hz, 12 Hz, H-6a and 4.54, dd, J = 2.1 Hz, 12 Hz, H-6b) and an anomeric proton linked to sulfur atom (δ_H 5.07, 1H, d, J = 8.9 Hz, H-1). The ^{13}C NMR showed carbon signals analogous to oxygenated sp2 methine carbons (δ_C 83.64, 80.56, 73.35 and 71.85), a methylene carbon (δ_C 63.38) and an anomeric carbon (δ_C 93.06). The large coupling constant shown by anomeric proton at δ_H 5.07 (J = 8.9 Hz) suggested the β- configuration of the compound. ESIMS gave the pseudomolecular ion peak at *m/z* 265.062 $[M+Na]^+$, corresponding to the elemental formula of $C_7H_{14}Na\ O_5S_2$, *m/z* 265.0175. These spectroscopic data closely resembled to those of methyl-1-thio-β-D-glucopyranosyl disulfide, published earlier (Cha et al., 2018). EIMS showed fragmentation peak at 163 which confirmed the presence of disulfide-methyl group (-$SSCH_3$, formula weight: 79). These results proved that compound **6** is methyl-1-thio-β-D-glucopyranosyl disulfide.

3.6 Structure elucidation of compound 7

Compound **7** appeared as colorless crystals which displayed six signals in ^{13}C NMR spectra, five peaks relating to the aromatic carbons (δ_C 154.69, 152.46, 137.22, 125.0 and 123.31) and one for a methylene carbon connected to hydroxyl group (δ_C 65.22). ^1H NMR showed three peaks at δ_H 8.01 (1H, d, J = 3 Hz), 7.36 (1H, J = 9 Hz) and 7.233 (1H, dd, J = 3.6 Hz, 5.4 Hz), which are associated with protons of aromatic carbons and an additional peak at δ_H 4.579 (2H, s) representing a methylene protons attached to a quaternary carbon and hydroxyl group. The number and position of signals in ^1H and ^{13}C traced the presence of two quaternary

carbons in the compound. Likewise EIMS data showed fragmentation peaks at 124, 108, 68 and 52 which indicated the prevalence of hydroxyl group, methylene hydroxyl group and nitrogen in the molecule. From the above results and the literature (Guo et al., 2013; Liu et al., 2013; Su et al., 2016), the compound was identified as 5-hydroxy-2-pyridinemethanol.

3.7 Structure elucidation of compound 8

Compound **8** was obtained as colorless semisolid and its ^{1}H NMR, ^{13}C NMR and ESIMS results resembled to that of 2-deoxyribonolactone reported earlier (Kitajima et al., 1999; Miranda et al., 2004). The ^{13}C NMR results depicted a five carbon compound with presence of carboxy group (δ_C 178.63, C-1), one methylene (δ_C 39.15, C-2) and three oxygenated methylene carbons (δ_C 64.51, C-570.14, C-3 and 91.17, C-4). Similarly ^{1}H NMR supported the existence of hydroxymethylene protons [δ_H 3.68 (1H, dd, J = 2.8 Hz, 12.4 Hz) and 3.75 (1H, dd, J = 4.1 Hz, 12.4 Hz)] and methylene protons [δ_H 2.36 (1H, dd, J = 2.75 Hz, 17.85 Hz) and 2.905 (1H, dd, J = 6.9Hz, 17.85 Hz)]. ESIMS provided the molecular ion peak at m/z 155.0138 $[M + Na]^+$, conforming the elemental formula of $C_5H_8NaO_4$, 155.0135. The optical rotation was determined to be 0.127 (c 0.013, CH_3OH). By comparing the spectral data and polarity of the compound with the previously published result by Miranda et al., 2004, the compound was confirmed as (3S, 4R)-2-deoxyribonolactone.

3.8 Identification of compound 9

Compound **9** was obtained as amorphous white solid. Signals at δ_H 1.56 (2H, m), 1.40 (2H, m) and 0.99 (3H, t) in ^{1}H NMR, likewise the peaks at δ_C 33.32, 20.21 and 14.33 in ^{13}C NMR indicated the presence of propyl chain

terminating with –CH_3 group. ^{13}C NMR signals at δ_C 101.60, 71.53, 71.09, 70.55, 65.16 and 63.16 inferred the fructopyranose ring, which was further supported by ^1H NMR signals at δ_H 3.90 (1H, d, J = 9.6 Hz), 3.82 (1H, m), 3.77 (1H, dd, J = 4.6, 3.2 Hz), 3.74 (1H, dd, J= 4.2, 2.1 Hz), 3.73 (1H, d, J = 4.1 Hz), 3.69 (1H, d, J = 11.6 Hz), 3.64 (1H, dd, J = 12, 1.4 Hz). A triplet-duplet peak at δ_H 3.49 (2H, td, J = 9.2, 6.8 Hz) along with ^{13}C NMR peak at δ_C 61.23 indicated the presence of –CH_2 group associated with oxygen and alkyl group at C-1' position. Thus, *n*- butyl group was estimated to occur at C-1'. The large coupling constant confirmed the β-configuration of the butyl chain. From these results and literature (Lee, S.Y. et al., 2010; Pyo et al., 2006), the compound was known to be *n*-Butyl-β-D-fructopyranoside.

3.9 Identification of compound 10

Compound **10** was isolated as white crystals. Its ^1H and ^{13}C NMR spectra showed the signals similar to that observed for uridine (Kang et al., 2018). ^{13}C NMR spectrum exhibited nine carbon signals, four olefinic/ aromatic carbons (δ_C 157.12, 172.73, 103.01 and 141.83), a methylene carbon (δ_C 62.38) and four ribose carbons (δ_C 91.46, 75.79, 71.24 and 86.04). Proton signals at δ_H 3.828 (1H, dd, J = 2.4, 12.3 Hz) and 3.718 (1H, dd, J = 3.6, 14.4 Hz) signified the existence of methylene carbon of ribose unit while δ_H 7.69 (1H, d, J = 7.8 Hz) and 5.66 (1H, d, J = 7.2 Hz) represented aromatic protons. The rest signals at δ_H 5.87 (1H, d, J = 4.8 Hz), 4.16 (1H, t, J = 4.8, 9.6 Hz), 4.13 (1H, t, J = 4.8, 10.2 Hz) and 3.965 (1H, m) supported the ribose ring in the molecule. EIMS spectra evinced the presence of uracil moiety (*m/z* 111) and tetrahydrofuran ring (*m/z* 71). Ultimately the compound was recognized as uracil by comparing the TLC pattern of standard compound in the laboratory.

3.10 Identification of compound 4, 11, 12 and 13

Compound **4** was obtained as brown powder and was identified to be β-Sitosterol glucoside by comparing the TLC pattern with the reference compound.

Compound **11** was obtained as colorless syrup and it was identified as tagatose from the results of EIMS and comparing with reference β-D-fructopyranose.

Compound **12** which occurred was colorless syrup showed slightly difference in Rf value on TLC plate than compound **11** and β-D-fructopyranose. ^{13}C NMR exhibited six peaks at δ_C 105.20, 83.48, 78.73, 77.19, 64.71 and 61.51, which were similar to those exhibited by fructose derivatives. ^{1}H NMR showed signals at δ_H 4.90 (1H, d, J = 8.3 Hz) and 3.92 (1H, t, J = 15.1, 7.5 Hz) linked the presence of two oxygenated carbons, δ_H 3.69 (1H, s) and 3.63 (1H, s) indicated a methylene carbon attached to quaternary carbon and hydroxyl group, and δ_H 3.57 (1H, dd, J = 6.8, 11.6 Hz) and 3.52 (1H, dd, J = 6.6, 11.3 Hz) indicated a methylene carbon attached to –CH and -OH groups. These NMR data were similar to that of β-D-fructofuranose, reported previously (Zhang et al., 2009) and thus, compound **12** was identified as β-D-fructofuranose.

Compound **13** was identified as β-D-fructopyranose as it showed TLC pattern like that of standard β-D-fructopyranose and was obtained as viscous light yellow syrup confirming it to be a plant-derived sugar derivative.

4. Discussion

Different species of *Brassica* genus remain an essential part of human diet globally as they constitute health beneficial nutrients and phytochemicals such as glucosinolates, phenolics, carotenoids, tocopherols and ascorbic acid. *B. oleracea* represent the most consumed vegetable species of Brassica, where varieties like broccoli and cauliflower (var. *botrytis*), cabbage (var. *capitata*), kale (var. *acephala*), kohlrabi (var. *gongylodes*) and brussel sprouts (var. g*emmifera*) fall (Raiola et al., 2018; Šamec et al., 2017). Since multiple studies indicated disease prevention and health promoting properties of kohlrabi, in the current study, we have investigated the bioactive compounds that are obtainable in the plant.

The methanol extract of *B. oleracea* var. *gongylodes* (red kohlrabi tuber) was fractionated using CH_2Cl_2, EtOAc, *n*-BuOH and H_2O. Through repeated open column chromatography using SiO2, sephadex LH20 and RP18 gel as stationary phase, nine compounds (**1**, **4**-**13**) were isolated from the EtOAc fraction and two (**2**, **3**) were isolated from CH_2Cl_2 fraction, which were identified based on the spectral information, literature, and assessment of the spots developed by the compounds and their respective standard or reference on the TLC plates. Among these, three of the compounds (**1**, **2** and **3**) were the indole alkaloids. Compound **1** was identified as a new indole-6-O-glycoside, namely, 1-methoxyindole 3-carboxylic acid 6-O- β-D-glucopyranoside. The aglycone structure, 1-methoxyindole 3-carboxylic acid, was formerly isolated from *Isatis indigotica* (Yang et al., 2014) and was synthesized by Somie et al. (Somei et al., 2001). However glycoside derivative has not reported yet. Likewise **2** and **3** were indole 3-acetonitrile and 1-methoxyindole 3-acetonitrile,

which were known to occur in different cruciferous plants (Kim et al., 2004; Pedras et al., 2006; Wu et al., 2012; Yang et al., 2014). Aglycone of **1** (1-methoxyindole 3-carboxylic acid), **2** and **3** had potent inhibitory action on NO production induced by LPS (Yang et al., 2014) and **3** exhibited antifungal effect (Pedras et al., 2006) as well.

Compound **6**, methyl-1-thio-β-D-glucopyranosyl disulfide, was the major compound in red kohlrabi as it was isolated in large quantity (>200 mg). Reported earlier by Cha et al., 2018, **6** moderately inhibited LPS-induced NO production in BV2 cells, with IC_{50} value of 44.10 μM. **7** was found to have anti-obesity effect and with IC_{50} value of 93.57 ± 0.94 μM, it inhibited lipid accumulation in 3T3-L1 cells during adipocyte differentiation via suppression of transcriptional factors, including PPARγ, C/EBPα, and SREBP-1c, the adipogenesis related gene (ACC), and enzymes (FAS) (Oh et al., 2016).

From EtOAc fraction, other common compounds such as **4**, **8, 9**, **10**, **11**, **12** and **13** were also isolated. **4** was a phytosterol glucoside, β-Sitosterol glucoside, that had demonstrated multiple bioactivities such as angiogenic (Choi et al., 2002; Moon et al., 1999), antihyperglycemic via increase in insulin levels (Ivorra et al., 1988), anti-inflammatory (Prieto et al., 2006) and inhibition of breast cancer cells (Ju et al., 2004; Xu et al., 2018). It also exhibited its pharmaceutical potential as absorption enhancer of drugs through biological membrane via perturbation of paracellular and transcellular pathways (Maitani et al., 2000; Nakamura et al., 2002). An aliphatic glycoside, **9**, was also found to have anti-inflammatory effect (Xu et al., 2005).

Compound **5** was found to inhibit adipogenesis, signified by reduced mRNA expression of (PPARγ), fatty acid binding protein-4 (FABP4), C/EBPα and lipoprotein lipase (LPL), and also promote the osteogenic

differentiation, which was indicated by the increase in mRNA expression of molecular biomarkers of osteoblast such as alkaline phosphate, osteopontin (OPN), osteocalcin and collagen type 1 α1 in the rat bone mesenchymal cells (Tan et al., 2014). Anti-fungal property, against *Candida albicans* of **5** was also explored (Subramenium et al., 2018).

(3S, 4R)-2-deoxyribonolactone (**8**), which possesses oxa-cyclopentane ring as the prostaglandin E2 (PGE2) displayed effects related to PGE2 by inducing cFos mRNA, however, at higher concentrations, unlike PGE2, it did not enhanced tetradecanoyl phorbol acetate (TPA) induced HL-60 cells differentiation but rather antagonized the TPA-induced differentiation in a dose-dependent manner. In contrast, **8** was found non-toxic in MTT assay, thus signifying it to be safe for normal cells at optimized concentrations (Miranda et al., 2004).

An in vivo study found that dietary uridine, **10**, given along with choline and decahexanoic acid enhanced learning and memory improvement by increasing total brain phospholipids (Holguin et al., 2008). Uridine, isolated from *Pleurotus giganteus*, stimulated neurite outgrowth in vitro by inducing MEK/ ERK and PIP3K-Akt-mTOR mediated phosphorylation of cAMP respeonse element binding protein (CREB) and expression of growth associated protein 43 (Phan et al., 2015).

Three fructose derivatives, tagatose (**11**), β-D-fructofuranose (**12**) and β-D-fructopyranose (**13**) were also isolated. Tagatose is a rare natural hexoketose which attains application as a low calorie sweetener and as an additive detergents, cosmetics and pharmaceutical formulations (Oh, 2007). The sweet taste of kohlrabi can be attributed to the presence of these reducing sugars in relatively large amount.

5. Conclusion

Since different natural products have afforded health promoting and disease curing drugs, the phytochemical research for chemical diversity in pharmacological screening programs is drawing attention, particularly in edible sources worldwide. In this study, tuber of a minor crop, B. oleracea var. gongylodes, was extracted with methanol and fractionated with solvents of different polarity. Isolation of EtOAc fraction of methanol extract led to the finding of novel compound, as N-methoxy-6-hydroxyindole-3-carboxylic acid-6-O-β- D-glucopyranoside, **1**. In addition, bioactive compounds **2**, **3**, **4**, **5**, **6**, **7**, **8** and **9** were identified to occur in kohlrabi for the first time. Moreover, the components responsible for the anti-inflammatory activity of red kohlrabi extract that was identified in previous studies were uncovered through this study. The systemic isolation of a new compound and 12 known compounds could provide valuable chemical diversity in the existing pool of bioactive compounds from edible sources that can be used for further pharmacological investigations.

6. References

Agriculture, U.S.D.o., 2019. Kohlrabi, raw. https://fdc.nal.usda.gov/fdc-app.html#/food-details/168424/nutrients.

Ambrosone, C.B., Tang, L., 2009. Cruciferous vegetable intake and cancer prevention: role of nutrigenetics. Cancer Prevention Research 2(4), 298-300.

Bang, M.-H., Lee, D.-Y., Oh, Y.-J., Han, M.-W., Yang, H.-J., Chung, H.-G., Jeong, T.-S., Lee, K.-T., Choi, M.-S., Baek, N.-I., 2008. Development of biologically active compounds from edible plant sources XXII. Isolation of indoles from the roots of *Brassica campestris* ssp *rapa* and their hACAT inhibitory activity. Applied Biological Chemistry 51(1), 65-69.

Bednarek, P., Schneider, B., Svatoš, A., Oldham, N.J., Hahlbrock, K., 2005. Structural complexity, differential response to infection, and tissue specificity of indolic and phenylpropanoid secondary metabolism in *Arabidopsis* roots. Plant Physiology 138(2), 1058-1070.

Björkman, M., Klingen, I., Birch, A.N., Bones, A.M., Bruce, T.J., Johansen, T.J., Meadow, R., Mølmann, J., Seljåsen, R., Smart, L.E., 2011. Phytochemicals of Brassicaceae in plant protection and human health–Influences of climate, environment and agronomic practice. Phytochemistry 72(7), 538-556.

Cha, J.M., Kim, D.H., Lee, T.H., Subedi, L., Kim, S.Y., Lee, K.R., 2018. Phytochemical Constituents of *Capsella bursa-pastoris* and Their Anti-inflammatory Activity. Natural Product Sciences 24(2), 132-138.

Choi, S.-H., Ryu, D.-K., Park, S.-H., Ahn, K.-G., Lim, Y.-P., An, G.-H., 2010. Composition analysis between kohlrabi (*Brassica oleracea* var. *gongylodes*) and radish (*Raphanus sativus*). Horticultural Science & Technology 28(3), 469-475.

Choi, S., Kim, K.-W., Choi, J.-S., Han, S.-T., Park, Y.-I., Lee, S.-K., Kim, J.-S., Chung, M.-H., 2002. Angiogenic activity of β-sitosterol in the ischaemia/reperfusion-damaged brain of Mongolian gerbil. Planta Medica 68(04), 330-335.

Fischer, J., 1992. Sulphur-and nitrogen-containing volatile components of kohlrabi (*Brassica oleracea* var. *gongylodes* L.). Zeitschrift für Lebensmittel-Untersuchung und Forschung 194(3), 259-262.

Gross, D., Porzel, A., Schmidt, J., 1994. Phytoalexine mit Indolstruktur aus Kohlrabi {*Brassica oleracea* var. *gongylodes*)+/Indole phytoalexins from the kohlrabi (*Brassica oleracea* var. *gongylodes*)+. Zeitschrift für Naturforschung C 49(5-6), 281-285.

Guo, L.-n., Bai, J., Pei, Y.-h., 2013. Isolation and identification of the chemical constituents from *Rehmannia glutinosa* L. Journal of Shenyang Pharmaceutical University 7.

Holguin, S., Martinez, J., Chow, C., Wurtman, R., 2008. Dietary uridine enhances the improvement in learning and memory produced by administering DHA to gerbils. The FASEB Journal 22(11), 3938-3946.

Ivorra, M., D'ocon, M., Paya, M., Villar, A., 1988. Antihyperglycemic and insulin-releasing effects of beta-sitosterol 3-beta-D-glucoside and its

aglycone, beta-sitosterol. Archives Internationales de Pharmacodynamie et de Thérapie 296, 224-231.

Ju, Y.H., Clausen, L.M., Allred, K.F., Almada, A.L., Helferich, W.G., 2004. β-sitosterol, β-sitosterol glucoside, and a mixture of β-sitosterol and β-sitosterol glucoside modulate the growth of estrogen-responsive breast cancer cells in vitro and in ovariectomized athymic mice. The Journal of Nutrition 134(5), 1145-1151.

Jung, H.A., Karki, S., Ehom, N.-Y., Yoon, M.-H., Kim, E.J., Choi, J.S., 2014. Anti-diabetic and anti-inflammatory effects of green and red kohlrabi cultivars (*Brassica oleracea* var. *gongylodes*). Preventive Nutrition and Food Science 19(4), 281.

Kang, U., Ryu, S.M., Lee, D., Seo, E.K., 2018. Chemical Constituents of the Leaves of *Brassica oleracea* var. *acephala*. Chemistry of Natural Compounds 54(5), 1023-1026.

Kim, D.-b., Oh, J.-W., Shin, G.-H., Kim, Y.-H., Lee, J.S., Park, I.-J., Cho, J.H., Lee, O.-H., 2014. Inhibitory effect of kohlrabi juices with antioxidant activity on oxidative stress in human dermal fibroblasts (LB394). The FASEB Journal 28(1_supplement), LB394.

Kim, J.-S., Choi, Y.-H., Seo, J.-H., Lee, J.-W., Kim, Y.-S., Ryu, S.-Y., Kang, J.-S., Kim, Y.-K., Kim, S.-H., 2004. Chemical constituents from the root of *Brassica campestris* ssp *rapa*. Korean Journal of Pharmacognosy 35(3), 259-263.

Kitajima, J., Ishikawa, T., TANAKA, T., IDA, Y., 1999. Water-soluble constitutents of fennel. IX. glucides and nucleosides. Chemical and Pharmaceutical Bulletin 47(7), 988-992.

Kulkarni, A., Suzuki, S., Etoh, H., 2008. Antioxidant compounds from *Eucalyptus grandis* biomass by subcritical liquid water extraction. Journal of Wood Science 54(2), 153-157.

Lampe, J.W., Peterson, S., 2002. Brassica, biotransformation and cancer risk: genetic polymorphisms alter the preventive effects of cruciferous vegetables. The Journal of Nutrition 132(10), 2991-2994.

Lee, J.-W., Lee, D.-Y., Cho, J.-G., Baek, N.-I., Lee, Y.-H., 2010. Isolation and identification of sterol compounds from the red kohlrabi (*Brassica oleracea* var. *gongylodes*) sprouts. Journal of Applied Biological Chemistry 53(4), 207-211.

Lee, S.Y., Choi, S.U., Lee, J.H., Lee, D.U., Lee, K.R., 2010. A new phenylpropane glycoside from the rhizome of *Sparganium stoloniferum*. Archives of Pharmacal Research 33(4), 515-521.

Lee, Y.-J., Kim, J.-H., Oh, J.-W., Shin, G.-H., Lee, J.S., Cho, J.-H., Park, J.-J., Lim, J.-H., Lee, O.-H., 2014. Antioxidant and anti-adipogenic effects of kohlrabi and radish sprout extracts. Korean Journal of Food Science and Technology 46(5), 531-537.

Lim, T., 2014. *Brassica oleracea* (*Gongylodes* group), Edible Medicinal and Non Medicinal Plants. Springer, pp. 768-776.

Liu, Y., Feng, Z., Luo, W., Guo, Z., Deng, Z., Tu, X., Chen, J., Zou, K., 2013. The secondary metabolites from endophytic fungus *Penicillium* sp. of *Paris polyphylla* Sm. Tianran Chanwu Yanjiu Yu Kaifa 25(5), 585-589.

Luo, W., Zhao, M., Yang, B., Shen, G., Rao, G., 2009. Identification of bioactive compounds in *Phyllenthus emblica* L. fruit and their free radical scavenging activities. Food Chemistry 114(2), 499-504.

Maitani, Y., Nakamura, K., Suenaga, H., Kamata, K., Takayama, K., Nagai, T., 2000. The enhancing effect of soybean-derived sterylglucoside and β-sitosterol β-D-glucoside on nasal absorption in rabbits. International Journal of Pharmaceutics 200(1), 17-26.

Miranda, P.O., Estévez, F., Quintana, J., García, C.I., Brouard, I., Padrón, J.I., Pivel, J.P., Bermejo, J., 2004. Enantioselective Synthesis and Biological Activity of (3 S, 4 R)-and (3 S, 4 S)-3-Hydroxy-4-hydroxymethyl-4-butanolides in Relation to PGE2. Journal of Medicinal Chemistry 47(2), 292-295.

Montaut, S., Bleeker, R.S., 2010. Isolation and structure elucidation of 5′-O-β-d-glucopyranosyl-dihydroascorbigen from *Cardamine diphylla* rhizome. Carbohydrate Research 345(13), 1968-1970.

Moon, E.-J., Lee, Y.M., Lee, O.-H., Lee, M.-J., Lee, S.-K., Chung, M.-H., Park, Y.-I., Sung, C.-K., Choi, J.-S., Kim, K.-W., 1999. A ncovel angiogenic factor derived from Aloe vera gel: β-sitosterol, a plant sterol. Angiogenesis 3(2), 117-123.

Morales□Ríos, M., Joseph□Nathan, P., 1987. NMR studies of indoles and their N□carboalkoxy derivatives. Magnetic Resonance in Chemistry 25(10), 911-918.

Nakamura, K., Maitani, Y., Takayama, K., 2002. The enhancing effect of nasal absorption of FITC-dextran 4,400 by β-sitosterol β-D-glucoside in rabbits. Journal of Controlled Release 79(1-3), 147-155.

Oh, D.-K., 2007. Tagatose: properties, applications, and biotechnological processes. Applied Microbiology and Biotechnology 76(1), 1.

Oh, D.-R., Kim, Y., Choi, E.-j., Jung, M.-A., Bae, D., Jo, A., Kim, Y.R., Kim, S., 2016. Antiobesity effects of unripe *Rubus coreanus* Miquel and its constituents: An in vitro and in vivo characterization of the underlying mechanism. Evidence-Based Complementary and Alternative Medicine 2016.

Park, C.H., Yeo, H.J., Kim, N.S., Eun, P.Y., Kim, S.-J., Arasu, M.V., Al-Dhabi, N.A., Park, S.-Y., Kim, J.K., Park, S.U., 2017. Metabolic profiling of pale green and purple kohlrabi (*Brassica oleracea* var. *gongylodes*). Applied Biological Chemistry 60(3), 249-257.

Park, S.-Y., Lim, S.-H., Ha, S.-H., Yeo, Y., Park, W.T., Kwon, D.Y., Park, S.U., Kim, J.K., 2013. Metabolite profiling approach reveals the interface of primary and secondary metabolism in colored cauliflowers (*Brassica oleracea* L. ssp. *botrytis*). Journal of Agricultural and Food Chemistry 61(28), 6999-7007.

Park, W.T., Kim, J.K., Park, S., Lee, S.-W., Li, X., Kim, Y.B., Uddin, M.R., Park, N.I., Kim, S.-J., Park, S.U., 2012. Metabolic profiling of

glucosinolates, anthocyanins, carotenoids, and other secondary metabolites in kohlrabi (*Brassica oleracea* var. *gongylodes*). Journal of Agricultural and Food Chemistry 60(33), 8111-8116.

Pedras, M.S.C., Sarwar, M.G., Suchy, M., Adio, A.M., 2006. The phytoalexins from cauliflower, caulilexins A, B and C: Isolation, structure determination, syntheses and antifungal activity. Phytochemistry 67(14), 1503-1509.

Phan, C.-W., David, P., Wong, K.-H., Naidu, M., Sabaratnam, V., 2015. Uridine from *Pleurotus giganteus* and its neurite outgrowth stimulatory effects with underlying mechanism. PloS One 10(11).

Podsędek, A., 2007. Natural antioxidants and antioxidant capacity of *Brassica* vegetables: A review. LWT-Food Science and Technology 40(1), 1-11.

Prieto, J.M., Recio, M.C., Giner, R.M., 2006. Anti-inflammatory activity of β-sitosterol in a model of oxazoloneinduced contact-delayed-type hypersensitivity. Boletín Latinoamericano y del Caribe de Plantas Medicinales y Aromáticas 5(3), 57-62.

Pyo, M.-K., YunChoi, H.-S., Kim, Y.-K., 2006. Isolation of n-Butyl-β-D-fructopyranoside from *Gastrodia elata* Blume. Natural Product Sciences 12(2), 101-103.

Raiola, A., Errico, A., Petruk, G., Monti, D.M., Barone, A., Rigano, M.M., 2018. Bioactive compounds in Brassicaceae vegetables with a role in the prevention of chronic diseases. Molecules 23(1), 15.

Šamec, D., Pavlović, I., Salopek-Sondi, B., 2017. White cabbage (*Brassica oleracea* var. *capitata* f. *alba*): botanical, phytochemical and pharmacological overview. Phytochemistry Reviews 16(1), 117-135.

Sharma, I., Aaradhya, M., Kodikonda, M., Naik, P.R., 2015. Antihyperglycemic, antihyperlipidemic and antioxidant activity of phenolic rich extract of *Brassica oleraceae* var. *gongylodes* on streptozotocin induced Wistar rats. SpringerPlus 4(1), 212.

Somei, M., Tanimoto, A., Orita, H., Yamada, F., Ohta, T., 2001. Syntheses of Wasabi phytoalexin (methyl 1-methoxyindole-3-carboxylate) and its 5-iodo derivative, and their nucleophilic substitution reactions. Heterocycles 54(1), 425-432.

Su, H., Yang, H., Meng, C., Peng, C., Guo, L., Dai, O., 2016. Study on chemical constituents of seeds of *Croton tiglium* and their cytotoxicities. Zhongguo Zhong yao za zhi= Zhongguo zhongyao zazhi= China Journal of Chinese Materia Medica 41(19), 3620-3623.

Subramenium, G.A., Swetha, T.K., Iyer, P.M., Balamurugan, K., Pandian, S.K., 2018. 5-hydroxymethyl-2-furaldehyde from marine bacterium *Bacillus subtilis* inhibits biofilm and virulence of *Candida albicans*. Microbiological Research 207, 19-32.

Tan, X.-l., Zhang, Y.-H., Cai, J.-P., Zhu, L.-H., Ge, W.-J., Zhang, X., 2014. 5-(Hydroxymethyl)-2-furaldehyde inhibits adipogenic and enhances osteogenic differentiation of rat bone mesenchymal stem cells. Natural Product Communications 9(4), 1934578X1400900427.

Wu, Q., Bang, M.-H., Lee, D.-Y., Cho, J.-G., Jeong, R.-H., Shrestha, S., Lee, K.-T., Chung, H.-G., Ahn, E.-M., Baek, N.-I., 2012. New indoles from the roots of *Brassica rapa* ssp. *campestris*. Chemistry of Natural Compounds 48(2), 281-284.

Xu, H., Li, Y., Han, B., Li, Z., Wang, B., Jiang, P., Zhang, J., Ma, W., Zhou, D., Li, X., 2018. Anti-breast-Cancer Activity Exerted by β-Sitosterol-d-glucoside from Sweet Potato via Upregulation of MicroRNA-10a and via the PI3K–Akt Signaling Pathway. Journal of Agricultural and Food Chemistry 66(37), 9704-9718.

Xu, J., Li, X., Zhang, P., Li, Z.-L., Wang, Y., 2005. Antiinflammatory Constituents from the Roots of *Smilax bockii* warb. Archives of Pharmacal Research 28(4), 395-399.

Yang, L., Wang, G., Wang, M., Jiang, H., Chen, L., Zhao, F., Qiu, F., 2014. Indole alkaloids from the roots of *Isatis indigotica* and their inhibitory effects on nitric oxide production. Fitoterapia 95, 175-181.

Yang, M.-J., Cha, S.-S., Lee, J.-J., 2015. Effects of purple kohlrabi (*Brassica oleracea* var. *gongylodes*) flesh and peel ethanol extracts on the antioxidant activity and antiproliferation of human cancer cells. The Korean Journal of Community Living Science 26(2), 405-414.

Yi, M.-R., Kang, C.-H., Bu, H.-J., 2017. Antioxidant and anti-inflammatory activity of extracts from kohlrabi (*Brassica Oleracea* var. *Gonglodes*). Journal of the Korean Applied Science and Technology 34(2), 189-202.

Zhang, Z., Wang, D., Zhao, Y., Gao, H., Hu, Y.-H., Hu, J.-F., 2009. Fructose-derived carbohydrates from *Alisma orientalis*. Natural Product Research 23(11), 1013-1020.

ACKNOWLEDGEMENT

This study would not have been possible without the support, endurance and guidance of the following ones. It is to them who I owe my deepest gratitude.

I shall remain indebted to Prof. Jae Sue Choi and Prof. Hyeung Rak Kim, Department of Food and Life Science, Pukyong National University for their invaluable and persistent guidance in this work and giving me permission for accessing to use the laboratory and allowing to conduct this research work.

My sincere gratitude goes to Emeritus Prof. Taek Jeong Nam for sharing his pool of knowledge and providing handful of advices to reach the target research. I am grateful to Prof. Hyun Ah Jung, Department of Food Science and Human Nutrition, Jeonbuk National University, Jeonju for her assistance and encouragement throughout the course.

I extend my special thanks and appreciation to Dr. Su Hui Seong, PhD and Dr. Pradeep Paudel, PhD, for their immense support during my dissertation work. I feel extremely fortunate to have warmhearted and uplifting lab members, namely Se Eun Park, Bandana Manandhar, Grishma Bhattarai, Aditi Wagle and Srijan Shrestha, all of who have made my period of Masters' degree enjoyable and memorable.

Last, but not the least, my heartfelt thanks to everyone at Pukyong National University and all others who had directly and indirectly contributed in any form towards the successful completion of the dissertation.